Acyl-Coenzyme A Binding Protein Expression Alters Liver Fatty Acyl-Coenzyme A Metabolism†

Huan Huang,‡ Barbara P. Atshaves,‡ Andrey Frolov,‡ Ann B. Kier,§ and Friedhelm Schroeder*,‡

Department of Physiology and Pharmacology, Texas A&M University, College Station, Texas 77843-4466, and Department of Pathobiology, Texas A&M University, College Station, Texas 77843-4467

Received October 15, 2004; Revised Manuscript Received June 8, 2005

ABSTRACT: Although studies in vitro and in yeast suggest that acyl-CoA binding protein ACBP may modulate long-chain fatty acyl-CoA (LCFA-CoA) distribution, its physiological function in mammals is unresolved. To address this issue, the effect of ACBP on liver LCFA-CoA pool size, acyl chain composition, distribution, and transacylation into more complex lipids was examined in transgenic mice expressing a higher level of ACBP. While ACBP transgenic mice did not exhibit altered body or liver weight, liver LCFA-CoA pool size increased by 69%, preferentially in saturated and polyunsaturated, but not monounsaturated, LCFA-CoAs. Intracellular LCFA-CoA distribution was also altered such that the ratio of LCFA-CoA content in (membranes, organelles)/cytosol increased 2.7-fold, especially in microsomes but not mitochondria. The increased distribution of specific LCFA-CoAs to the membrane/organelle and microsomal fractions followed the same order as the relative LCFA-CoA binding affinity exhibited by murine recombinant ACBP: saturated > monounsaturated > polyunsaturated C14−C22 LCFA-CoAs. Consistent with the altered microsomal LCFA-CoA level and distribution, enzymatic activity of liver microsomal glycerol-3-phosphate acyltransferase (GPAT) increased 4-fold, liver mass of phospholipid and triacylglyceride increased nearly 2-fold, and relative content of monounsaturated C18:1 fatty acid increased 44% in liver phospholipids. These effects were not due to the ACBP transgene altering the protein levels of liver microsomal acyltransferase enzymes such as GPAT, lysophosphatidic acid acyltransferase (LAT), or acyl-CoA cholesterol acyltransferase 2 (ACAT-2). Thus, these data show for the first time in a physiological context that ACBP expression may play a role in LCFA-CoA metabolism.

Intracellular long-chain fatty acids (LCFAs)[1] are rapidly acylated to long-chain fatty acyl-CoAs (LCFA-CoAs) which are classically considered substrates in diverse intracellular metabolic pathways for energy production (mitochondrial oxidation), formation of storage lipids (triacylglycerides, cholesteryl esters), and phospholipid synthesis for membrane biogenesis (*1*−*5*). However, growing evidence indicates that LCFA-CoAs not only serve as metabolic intermediates but are required for glucose uptake (*6*−*12*), protein trafficking (*13*), vesicular trafficking (*14*−*18*), intracellular signaling (*2*, *19*), and regulation of DNA transcription (*20*−*24*). LCFA-CoAs are active LCFA metabolites that, at low levels, are believed to facilitate insulin-mediated glucose uptake and utilization but, at higher levels, inhibit insulin action (*6*−*12*).

Liver expresses several classes of soluble, intracellular LCFA-CoA binding proteins including acyl-CoA binding protein (ACBP), liver fatty acid binding protein (L-FABP), and sterol carrier protein 2 (SCP-2) (*1*, *2*). These LCFA-CoA binding proteins differ markedly in concentration, intracellular distribution, and affinities and specificity for LCFA-CoAs. Relative concentrations of these proteins in liver are in the order L-FABP ≥ ACBP ≫ SCP-2. SCP-2 is highly localized in peroxisomes and not found in nuclei (*1*). Although L-FABP and ACBP are both primarily cytosolic (*1*, *25*), low concentrations are present in nuclei where these proteins interact with nuclear peroxisome proliferator activated receptor α (PPARα) (*26*−*28*) and hepatocyte nuclear factor 4α (HNF4α) (*29*), respectively. Despite these similarities in intracellular distribution, however, the affinities of L-FABP and ACBP for LCFA-CoAs differ markedly. ACBP binds C_{14} to C_{22} LCFA-CoAs with very high affinity, K_ds ≤ 0.5 nM (*30*−*32*). In contrast, L-FABP exhibits 30−2000-fold weaker LCFA-CoA binding affinities (*2*, *33*). Finally, among these intracellular LCFA-CoA binding proteins, only ACBP appears to exclusively bind LCFA-CoAs, while L-FABP and SCP-2 are much more promiscuous, as evidenced by interaction with LCFAs and a host of other

† This work was supported in part by a grant from the National Institutes of Health, USPHS (DK41402).

* To whom correspondence should be addressed. Phone: (979) 862-1433. Fax: (979) 862-4929. E-mail: fschroeder@cvm.tamu.edu.

‡ Department of Physiology and Pharmacology, Texas A&M University.

§ Department of Pathobiology, Texas A&M University.

[1] Abbreviations: ACAT-2, acyl-CoA cholesterol acyltransferase 2; ACBP, acyl-CoA binding protein; ACS, acyl-CoA synthetase; CAT I, microsomal carnitine acyltransferase I; CPT I, carnitine palmitoyltransferase I; GPAT, glycerol-3-phosphate acyltransferase; HNF4α, hepatocyte nuclear factor 4α; LAT, lysophosphatidic acid acyltransferase; LCFA, long-chain fatty acid; LCFA-CoA, long-chain fatty acyl-CoA; L-FABP, liver fatty acid binding protein; PBS, phosphate-buffered saline; PPAR, peroxisome proliferator activated receptor; SCP-2, sterol carrier protein 2; SDS−PAGE, sodium dodecyl sulfate−polyacrylamide gel electrophoresis; SUV, small unilamellar vesicles; TBS, 10 mM Tris (pH 8.0) and 150 mM NaCl; TBST, Tris (pH 8.0), 150 mM NaCl, and 0.05% Tween 20.

10.1021/bi0477891 CCC: $30.25
Published on Web 07/12/2005

xenobiotic ligands (*2*, *33*, *34*). On the basis of these data, ACBP appears to be the major, high-affinity LCFA-CoA binding protein in liver where it specifically binds LCFA-CoAs (*1*, *2*, *19*).

In vitro studies suggest that ACBP may play competing roles in altering LCFA-CoA pool size and distribution. First, ACBP may increase the total cellular level (pool size) of LCFA-CoA by enhancing synthesis and preventing degradation. The cellular level (pool size) of LCFA-CoAs is determined in part by the relative activities of LCFA-CoA synthetase (ACS) (*35*) and LCFA-CoA consuming activities including acyltransferases and hydrolases (i.e., thioesterases) (*1*, *19*). In vitro data show that, while LCFA-CoAs partition readily into membranes ($K_p = 10^5$), ACBP extracts LCFA-CoAs from membranes to increase the soluble LCFA-CoA pool in vitro (*36*). By binding/extracting LCFA-CoA from membrane-associated ACS the ACBP is thought to enhance ACS activity by removing end-product inhibition (*19*, *35*, *37*). Concomitantly, LCFA-CoA binding to ACBP protects LCFA-CoAs from cellular LCFA-CoA hydrolases in vitro (*1*, *2*, *19*). Second, other in vitro data indicate that ACBP also enhances transfer of LCFA-CoAs to membranes/organelles for transacylation to glycerolipids and cholesteryl esters (endoplasmic reticulum) (*5*, *38*, *39*) or for oxidation (mitochondria, peroxisomes) (reviewed in refs *1* and *19*). While the variety of competing processes precludes simple a priori prediction of ACBP effects on LCFA-CoA pool size and distribution, a recent study with yeast indicates that ACBP overexpression increases total LCFA-CoA pool size 2-fold (*40*). However, the physiological relevance of these observations in mammalian tissues remains to be determined.

To begin to address these issues, in the present investigation ACBP transgenic mice were created wherein ACBP expression was increased but still within the range of physiological levels. Extraction and chemical analysis allowed determination of the effect of the ACBP transgene on mouse liver: (i) LCFA-CoA level, (ii) LCFA-CoA acyl chain composition, (iii) LCFA-CoA distribution, (iv) enzymes that transacylate LCFA-CoAs to form phosphatidic acid (GPAT, LAT), the precursor of phospholipids and neutral glycerides, as well as enzymes that transacylate cholesterol to form cholesteryl esters (ACAT-2), (v) liver lipid distribution, and (vi) acyl chain composition of liver glycerides (phospholipids, triacylglycerides).

MATERIALS AND METHODS

Materials. Protease inhibitor cocktail for mammalian tissues, alkaline phosphatase-conjugated goat anti-rabbit IgG, and 5-bromo-4-chloro-3-indolyl phosphate/nitroblue tetrazolium (BCIP/NBT) were purchased from Sigma-Aldrich (St. Louis, MO). Protein assay dye reagent concentrate was purchased from Bio-Rad Laboratories (Richmond, CA). Glycerol 3-phosphate, palmitoyl-CoA (C16:0-CoA), palmitoleoyl-CoA (C16:1-CoA), heptadecanoyl-CoA (C17:0-CoA), stearoyl-CoA (C18:0-CoA), oleoyl-CoA (C18:1-CoA), linoleoyl-CoA (C18:2-CoA), arachidoyl-CoA (C20:0-CoA), arachidonoyl-CoA (20:4-CoA), and chloroacetaldehyde (~50% solution in water) were obtained from Sigma-Aldrich. Docosahexaenoyl-coenzyme A (22:6-CoA) was generously provided by Dr. Eric Murphy (University of North Dakota). *cis*-Parinaric acid was obtained from Molecular Probes (Eugene, OR), and *cis*-parinaroyl-CoA was synthesized therefrom as described previously (*23*). Lipid reference mixture for thin-layer chromatography was obtained from Nu-Chek Prep (Elysian, MN). Silica gel G and Silica gel 60 thin-layer chromatography plates were purchased from Analtech (Newark, DE) and EM Industries, Inc. (Darmstadt, Germany), respectively. [1-^{14}C]Oleoyl-CoA was obtained from Perkin-Elmer Life and Analytical Sciences (Boston, MA). All other reagents were of the highest available grade.

Proteins and Antisera. Murine recombinant ACBP was purified, and rabbit polyclonal antisera to murine recombinant ACBP were produced as described earlier (*4*, *38*). Rabbit polyclonal antibody against glycerol-3-phosphate acyltransferase (GPAT) was kindly provided by Dr. Rosalind Coleman (Department of Nutrition, University of North Carolina, Chapel Hill, NC). Rabbit polyclonal antibody against lysophosphatidic acid acyltransferase (LAT) was a generous gift from Dr. Henry J. Pownall (Department of Medicine, Baylor College of Medicine, Houston, TX). Rabbit polyclonal antibody against acyl-CoA cholesterol acyltransferase-2 (ACAT-2), the predominant form of ACAT responsible for cholesterol esterification in liver, was obtained from Cayman Chemical (Ann Arbor, MI).

Creation of ACBP Transgenic Mice and Animal Care. FVB/N mice were used to generate heterozygous ACBP transgenic mice. Mice were fed standard mouse chow (Teklad Rodent Diet, W8604; Harlan Teklad, Madison, WI) ad libitum. The animals were kept on a constant light cycle of 12 h of light/12 h of dark. Mice in the facility were monitored quarterly for infectious diseases and were specific pathogen free, particularly in reference to mouse hepatitis virus. ACBP transgenic mice were produced by pronuclear injection on a FVB/N background according to standard protocols (*41*). In brief, mouse ACBP cDNA obtained as described earlier (*4*) was subcloned into the mammalian expression plasmid pKJ1DF (a generous gift from M. McBurney, University of Ottawa, Ottawa, Canada) using the unique restriction enzyme site *Xho*I. The *Eco*RI−*Hin*dIII fragment of the resultant construct including the phosphoglycerate kinase promoter region (P_{pgk}), the entire coding sequence of mouse ACBP, and a 3′ untranslated region (pgk 3′) was pronuclearly injected into mouse embryos, which were then transferred into pseudopregnant recipient mice to generate transgenic mice expressing ACBP. The presence of the transgene was verified by PCR screening and Western blot analysis. To ensure that any observed phenotypic changes were not the result of random ACBP cDNA insertion, eight transgenic strains were generated and screened. The Laboratory Animal Research Resources facility at Texas A&M University is AAALAC approved and staffed by a diplomate of the ACLAM. All animal protocols were approved by the Animal Care and Use Committee of Texas A&M University to ensure correct usage of the mice.

Liver Tissue Homogenization and Fractionation. Because acyl-CoA binding proteins such as ACBP are involved in fatty acid metabolism (e.g., oxidation, esterification), it seemed possible that ACBP transgenic mice might exhibit altered whole body phenotype (e.g., body weight, obesity). Since there were no significant differences in the body weights at early ages, the experiment was continued to determine if an alteration might be observed at older age. However, there was no difference in body weight between

the wild-type control and ACBP transgenic mice even at older mice aged 2 years. At that time, male ACBP transgenic and control mice were fasted overnight, weighed, and anesthetized (ketamine, 100 mg/kg; zylaxine, 10 mg/kg), blood was removed by cardiac puncture, and mice were euthanized by cervical dislocation under anesthasia according to a protocol (AUP no. 2003-269) approved by the Animal Care and Use Committee of Texas A&M University to ensure correct usage of the mice.

The mice were fasted for two reasons: (i) The liver LCFA-CoA level is influenced by nutritional status (reviewed in ref *1*). Since mice allowed access to chow ad libitum may vary in the amount of food consumed, it was more difficult to control liver levels of fatty acyl-CoA under this condition. Instead, fasting the mice overnight assured that the liver lipids were less influenced by when the mice last consumed food which can vary widely from animal to animal, and consequently the level of LCFA-CoA was more uniform between animals (*42*, *43*). (ii) When LCFA-CoA levels are low (i.e., at low molar ratios of LCFA-CoA:ACBP), ACBP is known to inhibit the activity of acyltransferase enzymes (*5*, *44*, *45*). Previous studies showed that fasting for 48 h increased the liver LCFA-CoA mass (*42*, *43*) and, as shown in the Results, the acyltransferase enzymes (e.g., GPAT) and phospholipid formation were not inhibited.

Livers were then harvested, weighed, divided into portions, snap-frozen on dry ice, and stored at −80 °C for subsequent fractionation, LCFA-CoA extraction, and Western blot analyses. For liver fractionation, liver samples were minced on ice, followed by homogenization with a motor-driven Teflon pestle. Homogenization was performed on ice in 0.4 mL of phosphate-buffered saline (PBS, pH 7.4) containing one Complete Mini Protease Inhibitor Cocktail Tablet (Roche Diagnostics Corp., Indianapolis, IN) per 10 mL of buffer. The tablet is a mixture of several protease inhibitors with broad specificity for the inhibition of serine, cysteine, and metalloproteases, as well as calpains. Cellular debris and nuclei were removed by sedimenting the homogenate at 600*g* and 4 °C for 10 min using an Eppendorf refrigerated microcentrifuge, 5417R (Brinkmann Co., Westbury, NY), with a standard fixed-angle rotor. The resulting low-speed supernatant [postnuclear supernatant (PNS)] was further fractionated by differential centrifugation (*39*) and sucrose gradient (*46*) into microsomal, mitochondria, and soluble cytosolic fractions as described earlier (*39*, *46*). The final centrifugation at 105000*g* and 4 °C for 60 min resulted in a sedimented fraction comprised of the microsomal fraction and a 105000*g* (105K) supernatant containing the soluble cytosolic fraction. The amount of protein in each fraction was quantified by the Bradford protein assay (Bio-Rad Laboratories) (*47*).

Western Blotting. The liver samples were subjected to sodium dodecyl sulfate−polyacrylamide gel electrophoresis (SDS−PAGE) separation (*48*). Western blotting of select proteins involved in LCFA-CoA metabolism was determined in the liver cytosolic fraction (ACBP), membrane fraction (LAT), and homogenate (GPAT, ACAT-2) as follows: Briefly, samples were prepared for electrophoresis by mixing with 5× sample loading buffer (4:1 v/v) containing glycerol, 2-mercaptoethanol, Tris-HCl, SDS, and Coomassie Brilliant Blue G-250. After heat denaturation (95 °C for 4 min) and brief centrifugation, the protein samples were loaded onto acrylamide gels (16% gel for ACBP, 12% gel for GPAT, LAT, and ACAT-2) (*49*). The gels were run at constant current, 30 mA per gel, until the blue dye ran off the gel. Proteins were then transferred from the polyacrylamide gels to nitrocellulose membranes at a constant voltage of 90 V and 4 °C for 2 h utilizing a Miniprotean II transblot apparatus (Bio-Rad Laboratories). The membranes were rinsed for 5 min in 10 mM Tris-HCl (pH 8.0), 150 mM NaCl, and 0.05% Tween 20 (TBST) three times. Nonspecific protein binding to the nitrocellulose was minimized by incubating the membranes in TBST and 3% gelatin for half an hour. The TBST/gelatin solution was removed, and the membranes were washed three times for 5 min each with TBST. The membranes were incubated with primary antibody overnight at room temperature with gentle shaking. The primary antibody solution was then removed, and the membranes were washed two times for 5 min each with TBST and two times for 5 min each with TBS. Alkaline phosphatase-conjugated secondary antibody (goat anti-rabbit IgG, 1:3000 dilution in TBS and 1% gelatin) was added to the membranes and the mixture allowed to incubate for 2 h at room temperature with gentle shaking. After removal of the secondary antibody solution, the membranes were washed two times for 5 min each with TBST and two times for 5 min each with TBS. The membranes were then washed for 5 min with alkaline phosphatase buffer [100 mM Tris-HCl (pH 9.0), 100 mM NaCl, and 5 mM $MgCl_2$]. Color development was initiated by the addition of alkaline phosphatase substrate (BCIP/NBT; Sigma). The reaction was stopped upon sufficient color development by washing the membranes with doubly distilled water. Membrane densitometry analysis was done utilizing a single-chip charge-coupled device video camera (FluorChemimager) and accompanying FluorChem image analysis software (version 2.0) from Alpha Innotech (San Leandro, CA). Protein quantification of ACBP was accomplished by comparing sample band intensity to that of a standard curve of the purified ACBP that had been processed under identical conditions and run on the same gel with the liver samples.

Fatty Acyl-CoA Chain Length Specificity of ACBP: Displacement of ACBP-Bound cis-Parinaroyl-CoA by Long-Chain Fatty Acyl-CoA. Murine recombinant ACBP binds *cis*-parinaroyl-CoA, a naturally occurring fluorescent LCFA-CoA with high affinity, $K_d = 7-12$ nM (*4*, *30*). This allowed the use of *cis*-parinaroyl-CoA displacement assay to determine the acyl chain specificity (i.e., carbon chain length, unsaturation) of the murine recombinant ACBP for naturally occurring, nonfluorescent LCFA-CoAs typically found in liver. The procedure was basically as described for L-FABP interaction with naturally occurring LCFA-CoAs (*33*), modified as follows: Briefly, ACBP (0.1 μM) in phosphate buffer (pH 7.4) was preincubated with *cis*-parinaroyl-CoA (0.085 μM) for 5 min at 24 °C to obtain maximal fluorescence. ACBP-bound *cis*-parinaroyl-CoA was displaced by addition of displacing fatty acyl-CoA (0.85 μM) with fatty acyl chain length ranging from 0 to 20 and 0−4 double bonds. These LCFA-CoAs included palmitoyl-CoA (C16:0-CoA), palmitoleoyl-CoA (C16:1-CoA), heptadecanoyl-CoA (C17:0-CoA), stearoyl-CoA (C18:0-CoA), oleoyl-CoA (C18:1-CoA), linoleoyl-CoA (C18:2-CoA), arachidoyl-CoA (C20:0-CoA), and arachidonoyl-CoA (20:4-CoA). The concentration of nonfluorescent, displacing LCFA-CoAs (i.e., 0.85 μM) was

far below the critical micellar concentration of these ligands (*1*, *50*). The fluorescence intensity of *cis*-parinaroyl-CoA (λ_{ex} = 310 nm, λ_{em} = 416 nm) was measured using a PC1 photon counting fluorometer (ISS, Champaign, IL). All fluorescence measurements were corrected for the blank (nonfluorescent LCFA-CoA ligand or protein only) and photobleaching.

Determination of Liver Long-Chain Fatty Acyl-CoA Content and Acyl Chain Distribution. Preparation of Sample for LCFA-CoA Extraction. For determination of LCFA-CoA content and distribution in liver homogenate, liver samples (about 50 mg) were minced with a razor blade and suspended in 1 mL of 100 mM KH_2PO_4 (pH 5.3). After addition of 50 pmol of the internal standard, heptadecanoyl-CoA (C17:0-CoA), the sample was homogenized for 20 s × 2 with a probe sonicator (energy level 3) with a Sonic Dismembrator, Model 550 (Fisher Scientific, Pittsburgh, PA). A 50 μL aliquot was removed and saved for protein analysis. For determination of LCFA-CoA content and distribution in the soluble fraction (cytosolic) of liver, liver samples (about 150 mg) were minced with a razor blade and suspended in 400 μL of homogenization buffer (pH = 5.3) in a 1.5 mL centrifuge tube. The buffer was chilled on ice to help keep tissue cold. Keeping the tissue on ice, the suspended minced tissue was homogenized with a motor-driven Teflon pestle. Then an additional 400 μL aliquot of the above homogenization buffer (pH = 5.3) was added before being transferred into centrifuge tubes and fractionated by differential centrifugation at 105000*g* and 4 °C for 60 min with a Sorvall RC M120 ultracentrifuge (Kendro Laboratory Products, Asheville, NC) with a fixed-angle rotor. Supernatant was carefully removed. A 650 μL aliquot of supernatant was mixed with 2 pmol of the internal standard, heptadecanoyl-CoA (C17:0-CoA), followed by addition of 100 mM KH_2PO_4 (pH = 5.3) to a final volume of 1 mL. The remaining supernatant was retained for protein analysis.

Solid-Phase LCFA-CoA Extraction. The following were added to the liver homogenate or 105000*g* supernatant samples described above: 2-propanol (1 mL), saturated $(NH_4)_2SO_4$ (0.13 mL), and acetonitrile (2.0 mL). The resultant emulsion was vortexed for 5 min and centrifuged at 3000*g* for 20 min. The supernatant was then removed and diluted with 100 mM KH_2PO_4 (pH = 5.3, 5 mL). For solid-phase extraction, an oligonucleotide purification cartridge (Applied Biosystems, Foster City, CA) was rinsed with acetonitrile (5.0 mL) and gently flushed with air. The cartridge was then washed with 25 mM KH_2PO_4 buffer (2.0 mL) and again gently flushed with air. The sample was then loaded in a polypropylene syringe and slowly pushed through the cartridge. The cartridge was flushed with 25 mM KH_2PO_4 (pH = 5.3, 5 mL), dried by flushing with air twice, and eluted slowly with 60% CH_3CN in 100 mM KH_2PO_4 (0.3 mL). The eluant containing the LCFA-CoA was collected in an amber HPLC vial.

Formation of Fluorescent LCFA-etheno-CoA Derivatives. Fluorescent LCFA-etheno-CoA derivatives were formed by reaction of standard LCFA-CoA solutions or liver LCFA-CoA extracts with chloroacetaldehyde reagent as described previously (*51*). Chloroacetaldehyde reagent was made to contain 1 M chloroacetaldehyde, 0.3 M citrate buffer, and 1% SDS, and the pH of the solution was adjusted to pH = 4. LCFA-CoA standards and liver LCFA-CoA extracts were reacted with equal volumes of the chloroacetaldehyde reagent at 85 °C for 20 min. The samples were then cooled and stored at 4 °C until ready for HPLC analysis (within 7 days).

Resolution of Fluorescent Long-Chain Acyletheno-CoA Derivativess by HPLC. Etheno-CoA samples were analyzed with a LUNA 150 × 2.0 mm phenylhexyl HPLC column with 3 μm particle size, together with a 4 × 2 mm phenylpropyl guard column (Phenomenex, Torrance, CA) as described previously (*51*) with minor modifications. The flow rate was 0.3 mL min^{-1}, and the temperature of the column was kept at 40 °C with a column-heating block. The mobile phase compositions were as follows: A, 1% acetic acid; B, 90% acetonitrile and 1% acetic acid; C, 0.25% triethylamine (TEA); D, 90% acetonitrile. The gradient elution profile was as follows: 0−10 min, 10% B and 90% A to 80% B and 20% A; 10−12 min, 80% B and 20% A to 80% C and 20% A; 12−15 min, 80% C and 20% A to 90% C and 10% D; 15−105 min, 90% C and 10% D to 70% C and 30% D; 105−106 min, 70% C and 30% D to 100% D; 106−115 min, 100% D; 115−117 min, 100% D to 10% B and 90% A; 117−120 min, 10% B and 90% A. All gradients were run under the linear setting. An equilibration time of 5 min was used between runs. The peaks were detected with a fluorescence detector. The excitation wavelength was set to 230 nm and the emission wavelength to 420 nm. Peak areas were integrated and quantified by reference to response factors calculated from separately injected standard mixtures and known concentrations of the internal standard heptadecanoyl-CoA (C17:0-CoA) added prior to extraction and derivatization as indicated above.

Because two LCFA-CoA peaks (i.e., 18:2-CoA, 20:4-CoA) coelute under the above gradient elution profile, these two peaks were separated using a modification of an established method (*52*) basically as follows [an Agilent Extend-C18 column (4.6 × 150 mm, 3.5 μm particle size) was used]: 0−5 min, flow rate 1 mL/min, 10% B and 90% A to 80% B and 20% A; 5−5.1 min, flow rate 1 mL/min, 80% B and 20% A to 80% C and 20% A; 5.1−7 min, flow rate reduced to 0.2 mL/min, 80% C and 20% A to 75% C and 25% D; 7−127 min, 75% C and 25% D; 127−157 min, flow rate 0.2 mL/min, 75% C and 25% D to 30% C and 70% D; 157−167 min, flow rate 0.2 mL/min, 30% C and 70% D to 100% D; 167−175 min, flow rate back to 1 mL/min, 100% D; 175−177 min, flow rate 1 mL/min, 100% D to 90% A and 10% B; 177−180 min, flow rate 1 mL/min, 90% A and 10% B. The equilibration time was 5 min between runs.

Liver Lipid Analysis. Lipid analysis was performed as previously described (*53*, *54*). Briefly, lipids from each liver homogenate were extracted by a hexane/2-propanol mixture (3:2 v/v) and centrifuged at 1500 rpm and 4 °C for 10 min. The extraction and centrifugation were repeated, and the two organic layers were pooled and dried under N_2. The residues were redissolved in 100 μL of chloroform and spotted onto silica gel G thin-layer chromatography plates. Individual lipid classes (cholesterol, free fatty acid, triacylglyceride, cholesteryl ester, and phospholipid) were separated on thin-layer chromatography (TLC) plates developed with a petroleum ether/diethyl ether/methanol/acetic acid (180:14:4:1 v/v) solvent system. Lipids were visualized in an iodine chamber, and lipid spots were scraped and quantitated by Marzo assay (*55*). Individual lipid classes were identified by comparison to a standard run in parallel lanes on the same TLC plates.

Lipid quantification was accomplished by comparison of the absorbance of the extracted homogenate lipid sample to the appropriate lipid standard curve. Protein concentration was determined by the method of Bradford (*47*) from the dried protein extract residue digested overnight in 0.2 M KOH. All glassware was washed with sulfuric acid−chromate before use.

Fatty Acid Composition of Phospholipids and Triacylglycerides. Fatty acid composition was analyzed by converting the lipid acyl chains to fatty acid methyl esters (FAMEs) as described previously (*53*). Briefly, lipids from liver homogenate were extracted with a hexane/2-propanol mixture (3:2 v/v) and separated on TLC plates along with the standards as described above. The phospholipid and triacylglyceride spots were scraped, and acid-catalyzed transesterification was performed. The FAMEs formed were then extracted into *n*-hexane and analyzed by gas−liquid chromatography on a Shimadzu (Kyoto, Japan) GLC-14A system equipped with a RTX-2330 capillary column (Restek, Bellefonte, PA) with 0.32 mm inner diameter and 30 m length. The injector and detector temperatures were both 260 °C. The temperature program was as follows: 100 °C for 1 min, 10 °C/min to 140 °C, 2 °C/min to 220 °C, hold for 1 min, and then ramp at 10 °C/min to 260 °C. Data were collected with a Waters SAT/IN analytical-to-digital interface, and data analysis was done with Millenium 32 3.2 software. Individual peaks were identified by comparison with known FAME standards (Nu-Chek Prep, Inc.), and quantitation was done with the internal standard 15:0 FAME.

Glycerol-3-phosphate Acyltransferase (GPAT) Activity. GPAT assay was performed essentially as described previously (*39*) with some modifications. Briefly, cell homogenate containing 50 μg of protein, 40 μM [1-^{14}C]oleoyl-CoA, and 0.735 mM glycerol 3-phosphate were incubated for 15 min at 37 °C in a shaking water bath. The reactions (total volume 0.1 mL) were performed in the presence of 80 mM NaF (phospatidate phosphohydrolase inhibitor) and 15 mM DTT in 70 mM Tris-HCl buffer (pH = 7.4). The mixture was extracted with 300 μL of a hexane/2-propanol mixture (3:2 v/v) followed by centrifugation for 2 min at top speed in a countertop centrifuge. The organic lipid layer was saved and the extraction repeated. The two organic fractions were pooled, dried under a stream of N_2, redissolved in 100 μL of chloroform, and spotted onto a silica gel 60 TLC plate. Phospholipids were separated by thin-layer chromatography using silica gel 60 plates (baked in a 100 °C oven overnight before use) in a solvent system containing chloroform/methanol/acetic acid/ddH_2O (50:37.5:3.5:2 v/v). The TLC plate was visualized in an iodine tank. The band corresponding to phosphatidic acid (R_f = 0.63, based on a phosphatidic acid standard) was scraped and counted using liquid scintillation counting.

Statistics. All results are expressed as the mean ± SE, with n = 8 for ACBP transgenic mice and n = 4 for control mice, unless otherwise stated. Statistical analysis was performed using a *t*-test with 95% confidence level (GraphPad Prism, San Diego, CA). Values with $p < 0.05$ were considered statistically significantly different.

RESULTS

ACBP Transgenic Mice Exhibit Increased Liver ACBP Protein Level. ACBP cDNA was subcloned into the mammalian expression plasmid pKJ1DF using the unique restriction enzyme site *Xho*I (Figure 1A) as described in Materials and Methods. The resultant construct was pronuclearly injected into mouse embryos, which were then transferred into pseudopregnant recipient mice to generate transgenic mice expressing ACBP. As indicated in Materials and Methods, eight strains of ACBP transgenic mice were generated to preclude the possibility that phenotypic alterations might be influenced by random insertion of the cDNA.

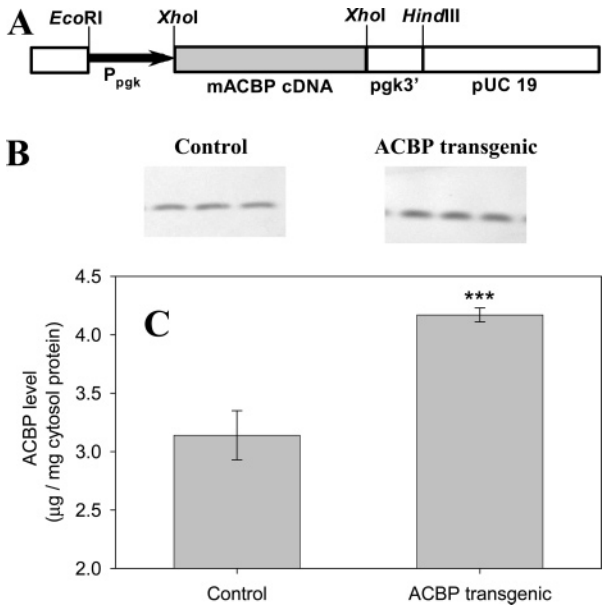

FIGURE 1: ACBP expression in ACBP transgenic mice. Panel A: Mouse expression construct. Mouse ACBP cDNA was subcloned into the mammalian expression plasmid pKJ1DF. The *Eco*RI−*Hin*dIII fragment of the resultant construct was pronuclearly injected into mouse embryos, which were then transferred into pseudopregnant recipient mice to generate transgenic mice expressing ACBP. Panel B: Representative Western blots of ACBP levels in livers of ACBP transgenic and control mice. Panel C: Quantitative analysis of ACBP levels from Western blots. Standards with a known amount of purified ACBP were run on each gel in panel B (data not shown) to construct the standard curve for quantitation. Values represent the mean ± SE (n = 8 for ACBP transgenic mice, n = 4 for control mice). An *** indicates significantly different from controls, $p < 0.001$.

To determine whether the expression of ACBP was in the physiological range, livers were then excised from both control and transgenic mice. Since ACBP is primarily a cytosolic protein, the 105K supernatant of each liver sample was subjected to SDS−PAGE followed by Western blotting with anti-ACBP antisera as demonstrated in representative Western blots (Figure 1B). For quantitation, standard amounts of murine recombinant ACBP protein (not shown) were included on each gel for densitometric analysis (Figure 1C) as described in Materials and Methods.

The basal level of ACBP in livers of control mice was 3.14 ± 0.21 (n = 4) μg of ACBP/mg of cytosolic protein (Figure 1C). The level of ACBP expression was visually higher in representative Western blots from livers of multiple ACBP transgenic mice as compared to that in livers of control mice (Figure 1B). This qualitative observation was confirmed by quantitative analysis showing 4.17 ± 0.06 (n = 8) μg of ACBP/mg of cytosolic protein in liver samples of ACBP transgenic mice. Thus, ACBP transgenic mice had 33% increased level of ACBP protein in liver. This level of

Table 1: Body Weight and Liver Weights of ACBP Transgenic and Control Mice[a]

gene type	sex	body wt (g)	liver wt (g)	liver wt/body wt
control	M	32.3 ± 3.3	1.42 ± 0.14	0.044 ± 0.003
	F	35.0 ± 3.2	1.73 ± 0.15	0.050 ± 0.002
ACBP transgenic	M	34.4 ± 2.8	1.77 ± 0.18	0.051 ± 0.002
	F	31.5 ± 2.2	1.60 ± 0.11	0.051 ± 0.004

[a] Values represent the mean ± SD (n = 4−6). M = male; F = female.

Table 2: Intracellular LCFA-CoA Distribution in Livers of ACBP Transgenic and Control Mice[a]

	LCFA-CoA level (pmol/mg of cell protein)		
cell fraction	control	ACBP transgenic	% change
homogenate	108.8 ± 11.2	183.8 ± 6.0***	+68.9
cytosol	2.25 ± 0.35	1.44 ± 0.08*	−36
membrane	106.55 ± 15.27	182.36 ± 8.61***	+71.1
membrane/cytosol	47/1	127/1	+170

[a] Values represent the mean ± SE (n = 4−8). *, ***: significantly different from controls (*, $p < 0.05$; ***, $p < 0.001$).

increased ACBP protein expression in liver was in the physiological range, i.e., in the same range as generated in response to high fat diet (*56*) or treatment with peroxisome proliferator agents (*57*, *58*).

Body and Liver Weight of ACBP Transgenic Mice. Since ACBP is thought to be involved in not only LCFA-CoA metabolism but also signaling and nuclear receptor regulation (reviewed in refs *1* and *2*), the possibility that ACBP transgenic mice might exhibit gross phenotype alterations was examined by comparison of body weight, liver weight, and the ratio of liver weight/body weight. Body weight, liver weight, and the ratio of liver weight/body weight of male control mice were 32.3 ± 3.3 g, 1.42 ± 0.14 g, and 0.044 ± 0.003, respectively (Table 1). Thus, liver weight comprised only about 4% of body weight. For male ACBP transgenic mice the body weight and liver weight were not significantly altered. The ratio of liver weight/body weight showed a slight increase in male ACBP transgenic mice; however, the changes were not statistically significant (Table 1). For female ACBP transgenic mice, body weight and liver weight were unaltered (Table 1). Thus, ACBP transgenic mice exhibited no or only slightly altered gross body phenotype, liver mass, or proportion of liver/body mass.

Liver LCFA-CoA Pool Size in ACBP Transgenic Mice. To test the possibility that ACBP transgenic mice exhibit altered total LCFA-CoA content of liver, the LCFA-CoA content was determined in livers from ACBP transgenic and control mice. The level of LCFA-CoA content in livers of control mice was 108.8 ± 11.2 pmol/mg of cell protein (Table 2). ACBP expression increased the content of LCFA-CoA in liver homogenate by nearly 70% ($p < 0.001$) to 183.8 ± 6.0 pmol/mg of cell protein. These data suggest for the first time that ACBP significantly increases LCFA-CoA pool size in a mammalian tissue in a physiological context.

Liver LCFA-CoA Distribution in ACBP Transgenic Mice. Although ACBP extracts LCFA-CoAs from membranes in vitro (*4*, *36*), it also donates bound LCFA-CoAs to model membranes in vitro (*4*) and to biological membranes/organelles for transacylation or oxidation in vitro (*1*, *5*, *19*, *38*, *39*). To determine the net result of these opposing actions in a more physiological context, the effect of ACBP expression on intracellular distribution of LCFA-CoAs between the membrane/organelle pool vs the soluble cytosolic pool of liver tissue was determined. Liver homogenates from control and ACBP transgenic mice were subjected to differential centrifugation to obtain a soluble, cytosolic fraction and a membrane/organelle fraction as described in Materials and Methods.

In control mice, the level of LCFA-CoA in membrane/organelle and cytosolic fractions was 108.8 ± 11.2 and 2.25 ± 0.35 pmol/mg of cell protein, respectively (Table 2). Thus, only about 2% of total LCFA-CoA was distributed to the cytosolic pool in livers of control mice. The liver LCFA-CoA was highly partitioned (47:1) in the membrane/organelle fraction as compared to the soluble/cytosolic pool. Livers of ACBP transgenic mice exhibited increased total LCFA-CoA pool by 1.7-fold ($p < 0.001$), but this increase was specific to the membrane/organelle-associated LCFA-CoA pool (Table 2). To determine if the increased LCFA-CoA pool size in the membrane/organelle fraction was reflected in membranes/organelles highly active in LCFA-CoA metabolism, microsomes and mitochondria were isolated from livers as indicated in Materials and Methods. Increased total LCFA-CoA pool size was observed in the microsomal, but not mitochondrial, fraction of livers from ACBP transgenic mice as compared to controls (Table 3). Interestingly, livers of ACBP transgenic mice exhibited decreased LCFA-CoA content of the soluble cytosolic fraction by 36% ($p < 0.05$, Table 2). Taken together, these studies demonstrated that ACBP transgenic mice not only had increased liver total LCFA-CoA pool size but specifically favored distribution of LCFA-CoA to the membrane/organelle fraction, especially microsomes, while concomitantly reducing LCFA-CoA appearing in the soluble/cytosolic fraction of the liver homogenate.

Liver Acyl Chain Content and Composition of the Total LCFA-CoA Pool in ACBP Transgenic Mice. Mouse liver LCFA-CoAs contained a diverse group of acyl chains. In control mouse livers, the mass of the LCFA-CoA pool was comprised primarily of LCFA-CoAs with C18 acyl chains (C18:2 > C18:1 ≫ C18:0 > C18:3), which together represented 61 pmol/mg of cell protein (Figure 2A). Two additional polyunsaturated LCFA-CoAs, C20:4 and C22:6, comprised 14.2 and 8.6 pmol/mg of cell protein, respectively (Figure 2A). The remaining LCFA-CoAs were comprised of C14, C16, C20, and C22 acyl chains, together accounting for 24.8 ± 1.5 pmol/mg of cell protein (Figure 2A). Analysis of the degree of unsaturation revealed that the mass of LCFA-CoAs in control livers was in the order polyunsaturated LCFA-CoAs > monounsaturated LCFA-CoAs > saturated LCFA-CoAs (Figure 2B). As compared to the control mouse liver, livers of ACBP transgenic mice exhibited significantly increased masses (pmol/mg of cell protein) of LCFA-CoAs with the following acyl chain lengths: C14:0, C16:0, C16:2, C18:0, C18:2, C18:4, C18:3, C20:3, and C22:6 (Figure 2A). Only the masses of C16:1-CoA, C18:1-CoA, C20:4-CoA, and C22:4-CoA were unaltered in livers of ACBP transgenic mice. There was no clear pattern of specific alterations in the longer chain vs shorter chain LCFA-CoAs in livers of ACBP transgenic mice. However, when the LCFA-CoAs were grouped according to acyl chain unsat-

Table 3: Microsomal and Mitochondrial LCFA-CoA Mass and Acyl Chain Distribution in Livers of ACBP Transgenic and Control Mice[a]

LCFA-CoA acyl chain	control		ACBP transgenic	
	mass (pmol/mg of protein)	%	mass (pmol/mg of protein)	%
		Microsome		
14:0	1.13 ± 0.31	19.5 ± 1.8	2.82 ± 0.42*	20.5 ± 1.8
16:0	0.41 ± 0.16	6.7 ± 1.0	1.30 ± 0.15*	8.9 ± 1.0
18:0	0.28 ± 0.12	4.4 ± 0.8	1.01 ± 0.05**	6.5 ± 0.8
20:0	0.11 ± 0.01	2.2 ± 0.6	0.52 ± 0.07**	3.4 ± 0.5
16:1	0.13 ± 0.04	2.3 ± 0.3	0.41 ± 0.09*	2.8 ± 0.3
18:1	0.74 ± 0.17	12.9 ± 0.5	2.22 ± 0.43*	15.0 ± 1.3
18:2	0.98 ± 0.21	17.3 ± 0.5	2.86 ± 0.49*	17.8 ± 1.4
20:3	0.08 ± 0.02	1.4 ± 0.1	0.29 ± 0.06*	1.9 ± 0.4
20:4	1.53 ± 0.28	27.2 ± 1.3	2.56 ± 0.46	17.1 ± 0.7**
22:6	0.36 ± 0.11	6.1 ± 0.6	0.91 ± 0.10*	6.1 ± 0.3
SAFA	1.94 ± 0.57	32.9 ± 1.9	5.66 ± 0.56**	39.3 ± 1.6*
MUFA	0.87 ± 0.21	15.1 ± 0.7	2.63 ± 0.50*	17.8 ± 1.4
PUFA	2.95 ± 0.61	52.0 ± 1.6	6.46 ± 1.2	42.8 ± 1.7*
total	4.9 ± 1.2		14.9 ± 2.0*	
		Mitochondia		
14:0	5.51 ± 0.23	7.12 ± 0.36	4.53 ± 0.74	6.37 ± 0.53
16:0	4.54 ± 0.31	5.95 ± 0.85	7.83 ± 0.99*	11.21 ± 0.71**
18:0	1.71 ± 0.14	2.19 ± 0.04	1.93 ± 0.24	2.82 ± 0.35
20:0	1.77 ± 0.17	2.26 ± 0.06	0.85 ± 0.11**	1.29 ± 0.25*
16:1	2.57 ± 0.12	3.31 ± 0.08	2.99 ± 0.61	4.17 ± 0.63
18:1	11.23 ± 0.29	14.53 ± 0.67	11.6 ± 1.6	16.8 ± 1.8
18:2	13.21 ± 0.72	17.1 ± 1.2	11.2 ± 1.8	15.8 ± 1.1
18:3	1.01 ± 0.09	1.31 ± 0.16	1.75 ± 0.30	2.48 ± 0.24*
20:3	1.61 ± 0.42	2.01 ± 0.42	1.21 ± 0.17	1.71 ± 0.11
20:4	28.7 ± 3.8	36.6 ± 2.7	19.7 ± 3.0	27.9 ± 1.6*
22:6	5.93 ± 0.52	7.60 ± 0.15	6.64 ± 0.84	9.50 ± 0.47*
SAFA	13.5 ± 0.4	17.5 ± 1.1	15.1 ± 1.6	21.7 ± 0.3**
MUFA	13.8 ± 0.4	17.8 ± 0.8	14.6 ± 2.2	20.9 ± 2.3
PUFA	50.5 ± 4.8	64.6 ± 1.8	40.5 ± 5.9	57.4 ± 2.5
total	77.8 ± 5.4		70.2 ± 8.6	

[a] Liver microsome and mitochondria were isolated as described in Materials and Methods. Data presented are the mean ± SE ($n = 3-5$). Abbreviations: SAFA, saturated fatty acyl chain; MUFA, monounsaturated fatty acyl chain; PUFA, polyunsaturated fatty acyl chain. *, **: significantly different from controls (*, $p < 0.05$; **, $p < 0.01$).

uration (Figure 2B), significant changes were observed. ACBP transgenic mice exhibited significantly increased mass of polyunsaturated LCFA-CoAs and somewhat that of saturated LCFA-CoAs but not monounsaturated LCFA-CoAs (Figure 2B). To determine if the increased LCFA-CoA mass distribution was reflected in membranes/organelles highly active in LCFA-CoA metabolism, the mass distributions of LCFA-CoAs from microsomes and mitochondria were analyzed (Table 3). The mass distribution of nearly all of the LCFA-CoA species measured were significantly increased in microsomes, but not mitochondria, of livers from ACBP transgenic mice (Table 3). For mitochondria, the only significant change observed for ACBP transgenic mice was slight increase in C16:0-CoA and decrease in C20:0-CoA (Table 3).

Since livers of ACBP transgenic mice exhibited increased total mass of LCFA-CoAs, it was important to determine whether this was reflected in the relative percent distribution of LCFA-CoAs, based on acyl chain length or acyl chain unsaturation. In control livers, C18:2-CoA alone accounted for 28.9% of total LCFA-CoA, and together the C18 acyl-CoAs comprised 53.5% of LCFA-CoAs while C20:4-CoA and C22:6-CoA represented 12.4% and 7.5% of LCFA-CoAs in control livers (Figure 3A). Further analysis showed that the longer chain LCFA-CoAs (i.e., C18, C20, C22) clearly predominated over the C14 and C16 acyl-CoAs (Figure 3A). When percent compositions were compared on the basis of degree of acyl chain unsaturation, the order of LCFA-CoA acyl chain distributions was again polyunsaturated LCFA-CoAs > monounsaturated LCFA-CoAs > saturated LCFA-CoAs (Figure 3B). ACBP transgenic mice exhibited 1.22-fold increased percent of polyunsaturated LCFA-CoAs (e.g., C18:2, C18:3, C18:4, C20:4, C22:6), primarily at the expense of nearly 2-fold decreased percent of monounsaturated LCFA-CoAs (e.g., C16:1, C18:1). With the exception of C18:0-CoA (Figure 3A), the liver LCFA-CoA pool of ACBP transgenic mice did not exhibit significantly altered overall percent of saturated LCFA-CoAs (Figure 3B). Analysis of the percent LCFA-CoA distribution revealed that the percent of C20:4 acyl-CoAs was decreased in microsomes from livers of ACBP transgenic mice (Table 3). Overall, the microsomal percent of saturated LCFA-CoAs increased, the percent of monounsaturated LCFA-CoAs was altered only slightly, and the percent of polyunsaturated LCFA-CoAs was decreased in microsomes from livers of ACBP transgenic mice. These changes in the LCFA-CoA acyl chain percent distribution pattern of microsomes reflected those observed with the membrane/organelle fraction from liver. For mitochondria of ACBP transgenic mice, there was a significant increase in percent C16:0-CoA; there was no significant change in monounsaturated acyl-CoAs; some of the percent polyunsaturated acyl-CoAs increased while others decreased, which resulted in no significant overall changes in polyunsaturated acyl-CoAs (Table 3).

In summary, regardless of whether the data were presented on a mass or percent basis, ACBP transgenic mice exhibited

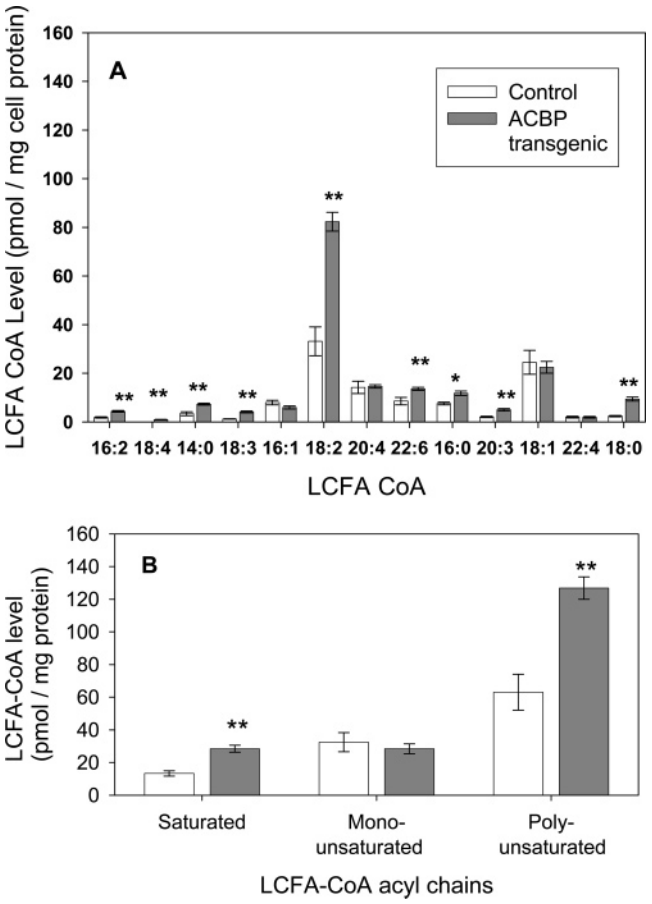

FIGURE 2: Total LCFA-CoA mass and LCFA-CoA acyl chain length and unsaturation in livers from ACBP transgenic and control mice. Open bars refer to control while solid bars refer to ACBP expressors. Panel A: Mass (pmol/mg of protein) content and distribution of liver LCFA-CoAs (plotted in the order of HPLC retention times) resolved by HPLC according to acyl chain length and degree of saturation. Values represent the mean ± SE ($n = 8$ for ACBP transgenic mice, $n = 4$ for control mice). Panel B: The mass of saturated, monounsaturated, and polyunsaturated LCFA-CoA classes was calculated from panel A for livers of ACBP transgenic and control mice. *, **: significantly different from controls (*, $p < 0.05$; **, $p < 0.01$).

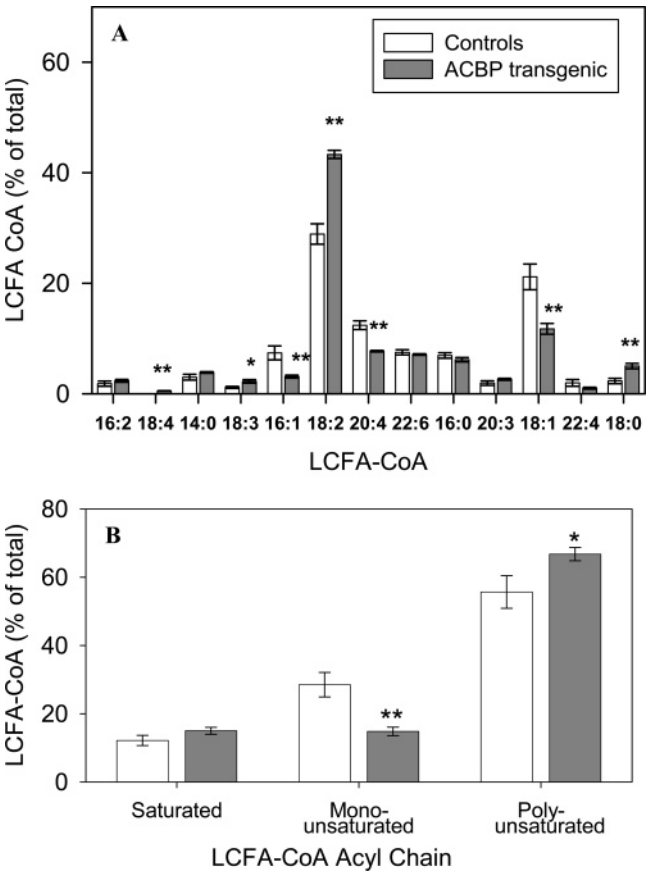

FIGURE 3: Percent acyl composition of total LCFA-CoAs in livers of ACBP transgenic and control mice. Panel A: Percent contribution of LCFA-CoAs with different chain length and degree of saturation (plotted in the order of HPLC retention times) to the total LCFA-CoA pool in livers of ACBP transgenic ($n = 8$) and control ($n = 4$) mice. Panel B: Percent contribution of saturated, monounsaturated, and polyunsaturated LCFA-CoA species. Open bars refer to control while solid bars refer to ACBP transgenic mice. Values represent the mean ± SE, with * and ** representing significantly different from controls (*, $p < 0.05$; **, $p < 0.01$).

significantly increased proportion of polyunsaturated LCFA-CoAs in livers.

LCFA-CoA Composition of the Liver 105K Supernatant from ACBP Transgenic Mice. As indicated in Table 2, the soluble/cytosolic fraction of liver contained only a small proportion (about 2%) of liver total LCFA-CoA. Since livers of ACBP transgenic mice had significantly increased the proportion of total polyunsaturated LCFA-CoAs, it was important to determine (i) whether the composition of the soluble/cytosolic LCFA-CoA pool was distinct from the total LCFA-CoA pool and (ii) if livers of ACBP transgenic mice also exhibit selectively increased proportion of polyunsaturated LCFA-CoAs in the soluble/cytosolic pool. Therefore, the soluble/cytosolic fraction was isolated from livers of control and ACBP transgenic mice and LCFA-CoA composition determined as described in Materials and Methods.

The LCFA-CoA acyl chain length composition of the soluble/cytosolic fraction (Figure 4A) differed significantly from that of the total liver LCFA-CoA pool (Figure 2A). When expressed on the basis of mass (i.e., pmol/mg of soluble protein), the order of acyl chain lengths in the soluble/cytosolic pool was as follows: C18:2 > C16:0 > C18:1 >20:4 > C16:1 (Figure 4A). Again as for the whole homogenate, the C20:4 and C22:6 LCFA-CoAs were present at small amounts representing 0.58 and 0.29 pmol/mg of soluble protein in the cytosolic fractions of livers from control mice. When the mass of LCFA-CoAs in control livers was compared on the basis of the degree of unsaturation, that of the soluble/cytosolic pool (polyunsaturated LCFA-CoAs ≫ monounsaturated LCFA-CoAs and saturated LCFA-CoAs; Figure 4B) also differed significantly from that of the liver total LCFA-CoAs (polyunsaturated LCFA-CoAs > monounsaturated LCFA-CoAs > saturated LCFA-CoAs; Figure 2B). The soluble/cytosolic fraction of livers from ACBP transgenic mice exhibited a significant and selective decrease in mass of the following specific acyl chains: C14:0, C16:0, C16:1, C18:0, C18:1, C20:4, and C22:6 (Figure 4A). The mass of the following LCFA-CoAs was not significantly altered in the liver soluble/cytosolic fraction of ACBP transgenic mice (C16:2, C18:2, C18:3, C18:4, and C20:2) (Figure 4A). When grouped on the basis of degree of unsaturation, ACBP transgenic mice exhibited significantly decreased mass of saturated and monounsaturated LCFA-CoAs but unaltered mass of polyunsaturated LCFA-CoA in the soluble/cytosolic LCFA-CoA pool from liver. When the

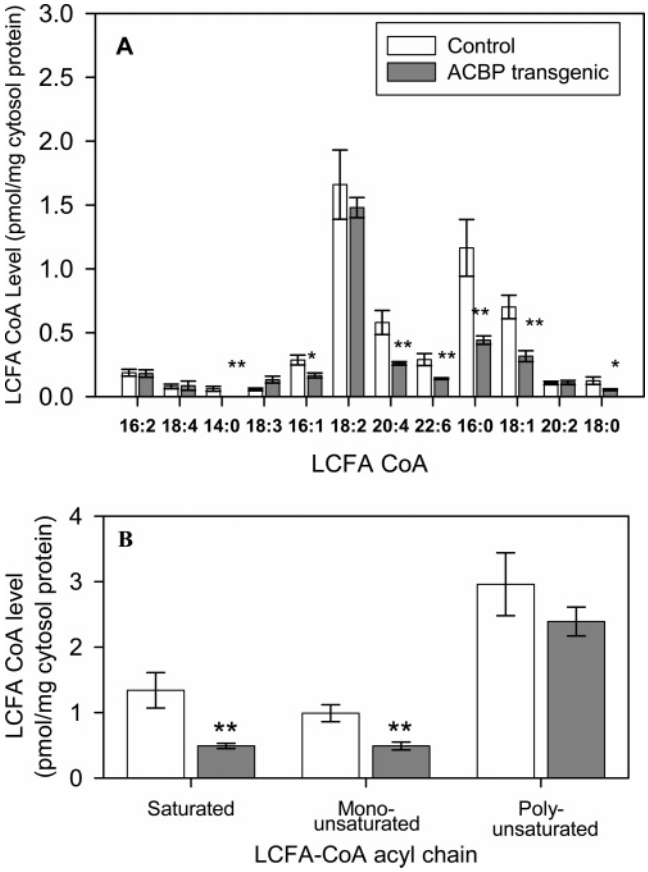

FIGURE 4: Total LCFA-CoA mass, acyl chain length, and acyl chain unsaturation in the soluble/cytosolic pool from livers of ACBP transgenic and control mice. The soluble/cytosolic fraction of liver homogenate was isolated as described in Materials and Methods. Open bars refer to control while solid bars refer to ACBP transgenic mice. Panel A: Mass (pmol/mg of protein) content and distribution of soluble/cytosolic LCFA-CoAs resolved by HPLC according to acyl chain length and degree of saturation (plotted in the order of HPLC retention times). Values represent the mean ± SE ($n = 8$ for ACBP transgenic mice, $n = 4$ for control mice). Panel B: The mass of saturated, monounsaturated, and polyunsaturated LCFA-CoA classes was calculated from panel A for the soluble/cytosolic fraction of livers from ACBP transgenic and control mice. *, **: significantly different from controls (*, $p < 0.05$; **, $p < 0.01$).

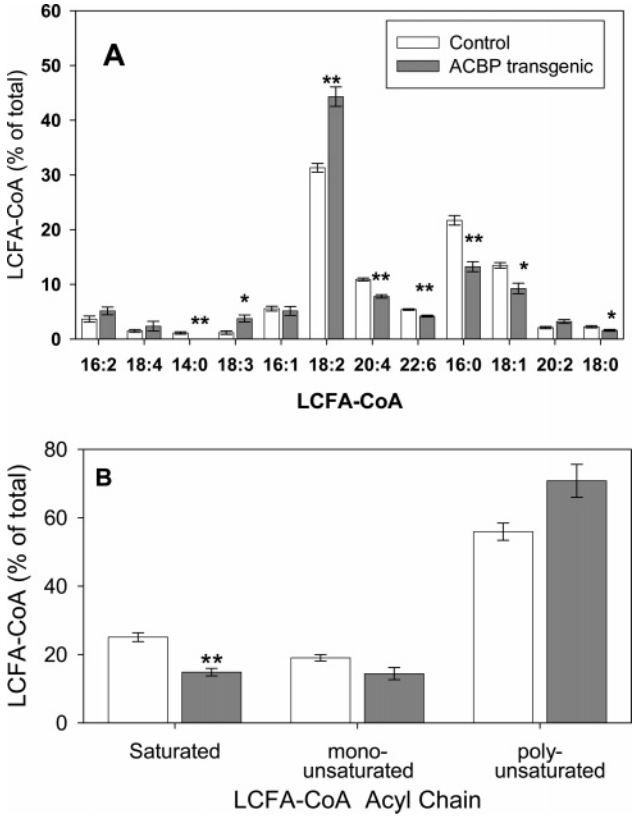

FIGURE 5: Percent acyl composition of LCFA-CoAs in the soluble/cytosolic pool from livers of ACBP transgenic and control mice. Panel A: Percent contribution of LCFA-CoAs with different chain length and degree of saturation (plotted in the order of HPLC retention times) to the soluble/cytosolic LCFA-CoAs in livers of ACBP transgenic ($n = 8$) and control ($n = 4$) mice. Panel B: Percent contribution of saturated, monounsaturated, and polyunsaturated LCFA-CoA species. Open bars refer to control while solid bars refer to ACBP transgenic mice. Values represent the mean ± SE, with * and ** representing significantly different from controls (*, $p < 0.05$; **, $p < 0.01$).

results were presented as percent composition, the soluble/cytosolic pool of livers from ACBP transgenic mice had significantly decreased the percent of saturated LCFA-CoAs (e.g., C14:0, C16:0, C18:0), basically unaltered percent of monounsaturated LCFA-CoAs (except decreased percent C18:1-CoA), and overall unaltered percent polyunsaturated LCFA-CoAs (decreased percent C20:4-CoA and percent C22:6-CoA was compensated by increased percent C18:2-CoA and percent C18:3-CoA).

In summary, these effects of the ACBP transgene on selectively reducing the mass of saturated and monounsaturated LCFA-CoAs in the liver soluble/cytosolic LCFA-CoA pool (Figure 4B) were in contrast to those in whole liver where ACBP transgenic mice exhibited increased mass of these types of LCFA-CoAs (Figure 2B). Likewise, the effects of the ACBP transgene on selectively reducing the percent of total saturated (but not total monounsaturated and total polyunsaturated) LCFA-CoAs in the soluble/cytosolic LCFA-CoA pool (Figure 5B) were in contrast to those in whole liver where ACBP transgenic mice exhibited unaltered percent of total saturated LCFA-CoAs but decreased and increased percent of total monounsaturated and total polyunsaturated LCFA-CoAs, respectively (Figure 3B).

ACBP Fatty Acyl-CoA Binding Specificities: Displacement Studies. The possibility that the effect of the ACBP transgene on LCFA-CoA mass, distribution, and composition reflected the relative affinity of mouse liver ACBP for specific LCFA-CoAs was considered. Therefore, recombinant mouse ACBP was isolated, and the relative abilities of naturally occurring LCFA-CoAs to displace a bound, naturally occurring fluorescent LCFA-CoA (*cis*-parinaroyl-CoA) were determined as described in Materials and Methods.

First, the effect of carbon chain length on the ability of saturated LCFA-CoAs to displace ACBP-bound *cis*-parinaroyl-CoA was examined (Table 4). Saturated LCFA-CoAs with 14−20 carbon chain length were good displacers (C20, C18, C16 > C14), medium-chain (e.g., C12, C10) saturated LCFA-CoAs displayed 4−16-fold lower affinity, and short-chain (e.g., C2−C8) saturated LCFA-CoAs as well as CoA itself did not displace bound *cis*-parinaroyl-CoA (Table 4). Thus, the ability of saturated LCFA-CoAs to displace bound *cis*-parinaroyl-CoA increased significantly with increasing chain length to achieve a maximum for C16−C20 LCFA-CoA (Table 4).

Second, the effect of acyl chain unsaturation on the ability of LCFA-CoAs to displace ACBP-bound *cis*-parinaroyl-CoA

Table 4: Displacement of ACBP-Bound *cis*-Parinaroyl-CoA by Naturally Occurring Fatty Acyl-CoAs[a]

displacing ligand	chain length	double bonds	displacement (%)
arachidoyl-CoA	C20	0	82.0 ± 1.5
stearoyl-CoA	C18	0	79.6 ± 0.8
palmitoyl-CoA	C16	0	72.1 ± 2.9
myristoyl-CoA	C14	0	46.6 ± 0.8
lauroyl-CoA	C12	0	20.8 ± 3.5
n-decanoyl-CoA	C10	0	4.9 ± 2.3
n-octanoyl-CoA	C8	0	0
n-hexanoyl-CoA	C6	0	0
N-butyryl-CoA	C4	0	0
acetyl-CoA	C2	0	0
CoA	C0	0	0
arachidonoyl-CoA	C20	4	53.4 ± 2.0
11,14,17-eicosatrienoyl-CoA	C20	3	71.2 ± 2.5
linolenoyl-CoA	C18	3	45.7 ± 1.0
linoleoyl-CoA	C18	2	55.9 ± 2.0
myristoleoyl-CoA	C14	1	28.7 ± 3.5

[a] ACBP (0.1 μM) was preincubated with *cis*-parinaroyl-CoA (0.085 μM), followed by addition of displacing fatty acyl-CoA (0.85 μM) as described in Materials and Methods. Values represent the mean ± SE ($n = 3-6$).

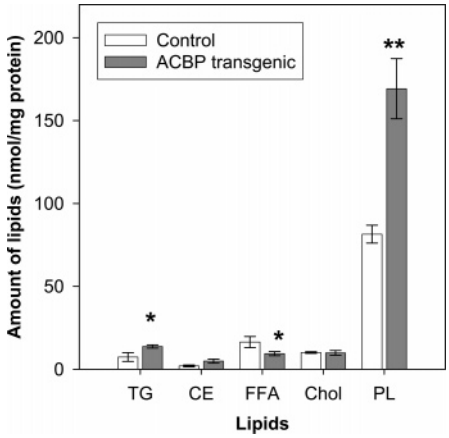

FIGURE 6: Lipid class distribution in livers of ACBP transgenic and control mice. Liver samples were extracted with organic solvents, and lipid class was separated by TLC as described in Materials and Methods. Open bars refer to control while solid bars refer to ACBP transgenic mice. The results (nmol/mg of protein) represent the mean ± SE ($n = 8$ for ACBP transgenic mice, $n = 4$ for control mice). Key: TG, triglyceride; CE, cholesteryl ester; FFA, free fatty acid; Chol, cholesterol; PL, phospholipids. *, **: significantly different from controls (*, $p < 0.05$; **, $p < 0.01$).

was determined (Table 4). All of the C14 to C20 unsaturated LCFA-CoAs tested displaced bound *cis*-parinaroyl-CoA but significantly ($p < 0.01$) less than the corresponding saturated acyl-CoAs (Table 4). The C14:1 myristoleoyl-CoA displaced bound *cis*-parinaroyl-CoA (28.7 ± 3.5%) significantly less than that by C14:0 myristoyl-CoA (46.6 ± 0.8%). The C18 and C20 unsaturated LCFA-CoAs also showed less displacement efficiency than the corresponding saturated C18:0 and C20:0 LCFA-CoAs (Table 4). Finally, when displacements by LCFA-CoAs of the same acyl chain length were compared, ACBP exhibited even weaker displacement by LCFA-CoAs with a greater number of double bonds (i.e., 2, 3, or 4) in the acyl chain.

Taken together, the above *cis*-parinaroyl-CoA displacement assay showed that ACBP readily bound LCFA-CoAs containing acyl chain lengths of C14 to C20. However, ACBP exhibited higher selectivity for saturated than unsaturated LCFA-CoAs as shown by greater *cis*-parinaroyl-CoA displacement than by saturated LCFA-CoAs.

Liver Lipid Class Distribution in ACBP Transgenic Mice. The lipid composition of livers from ACBP transgenic and control mice was determined after organic solvent extraction, resolution by TLC, and quantitation by chemical assay as described in Materials and Methods. The results showed that there was a 2-fold increase in phospholipid mass in livers of ACBP transgenic mice as compared to control mice (Figure 6). There was also a significant increase in the level of triacylglyceride (TG) and decrease in unesterified LCFA, while cholesterol and cholesterol ester levels remain unchanged (Figure 6). These data were consistent with ACBP transgenic mice exhibiting selectively enhanced formation of fatty acid containing glycerides (phospholipids and triacylglycerides) but not cholesteryl esters.

Liver Phospholipid Fatty Acid Composition in ACBP Transgenic Mice. Liver lipids were extracted and resolved by TLC as described in Materials and Methods. The phospholipid spots were hydrolyzed and converted to FAMEs and analyzed by gas liquid chromatography also as described in Materials and Methods. Figure 7 shows the fatty acid composition in terms of saturated (panel A), monounsaturated (panel B), and polyunsaturated (panel C) fatty acids. The biggest change observed in liver phospholipids from ACBP transgenic mice was a 44% increase in C18:1, a monounsaturated fatty acid (Figure 7). Liver phospholipids from ACBP transgenic mice exhibited modest alterations in the relative composition of several minor acyl chain components, i.e., decreased C22:0 and C20:0, decreased C18:3 and C20:2, and increased in C22:3. Although the liver lipids of young mice contain about 12% and 4% of C20:4 and C22:6 acyl chains, respectively (*59*), these acyl chains were either absent (C20:4) or present only in low amounts (C22:6) in the phospholipids of livers from the much older control and ACBP transgenic mice used herein (Figure 7). Taken together, these data suggest that liver phospholipid acyl chains of ACBP transgenic mice exhibited increased level of C18:1 while in general decreased percent composition of many of the very long chain LCFAs (C22:0, C24:0, C20:2).

Liver Triacyglyceride Fatty Acid Composition in ACBP Transgenic Mice. Liver lipids were extracted and resolved by TLC as described in Materials and Methods. Triacylglyceride spots were hydrolyzed and converted to FAMEs and analyzed by gas liquid chromatography as described in Materials and Methods. In triacylglycerides from livers of ACBP transgenic mice, the relative composition of saturated fatty acids such as C20:0 was increased while that of C24:0 was decreased, thereby resulting in unaltered percent composition of total saturated fatty acids (Figure 8A). With regard to the effect of ACBP transgene mice on triacylglyceride monounsaturated fatty acids (MUFAs), the only change noted was decreased C24:1, but there was no significant alteration in the percent composition of total MUFA (Figure 8B). For PUFA, there was an increase in C18:3, C20:2, and C22:2 and decrease in C22:3 and C22:6, but there was no change in the percent composition of total PUFA (Figure 8C). Polyunsaturated acyl chains such as C20:4 and C22:6 were absent or present only in low amounts, respectively, of the liver triacylglycerides of this age group of control and ACBP transgenic mice (Figure 8). Although the liver lipids of young

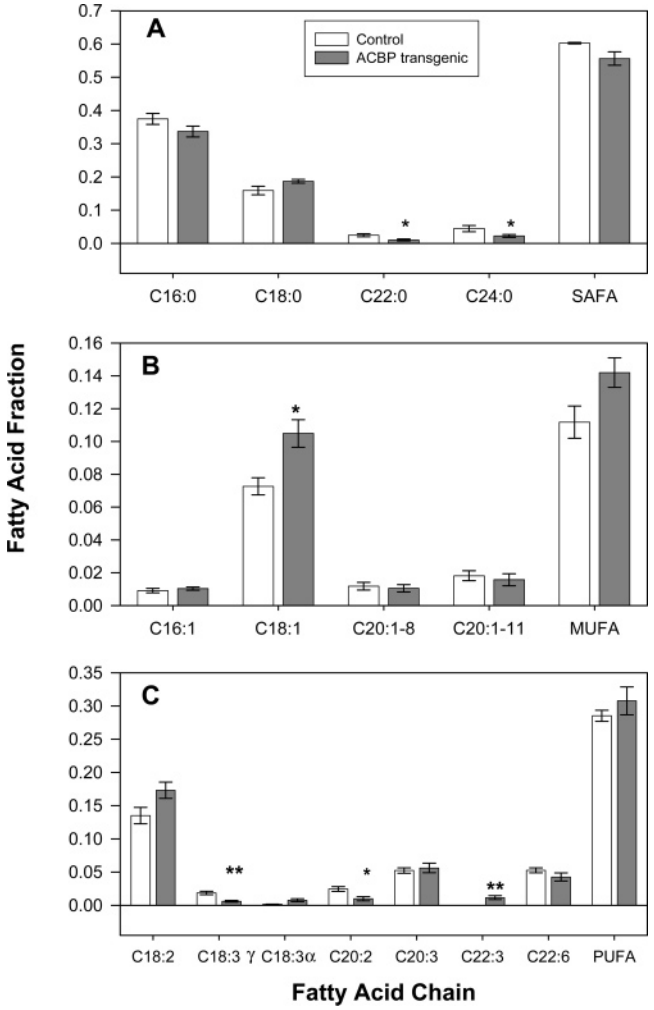

FIGURE 7: Fatty acid composition of phospholipids from livers of ACBP transgenic and control mice. Liver lipids were extracted and resolved by TLC. The phospholipid spots were hydrolyzed and converted to FAMEs and analyzed by gas chromatography as described in Materials and Methods. The results (mean ± SE; $n = 3-7$) are presented as fatty acid fractions. Panels: A, saturated fatty acids (SAFA); B, monounsaturated fatty acids (MUFA); C, polyunsaturated fatty acids (PUFA). *, **: significantly different from controls (*, $p < 0.05$; **, $p < 0.01$).

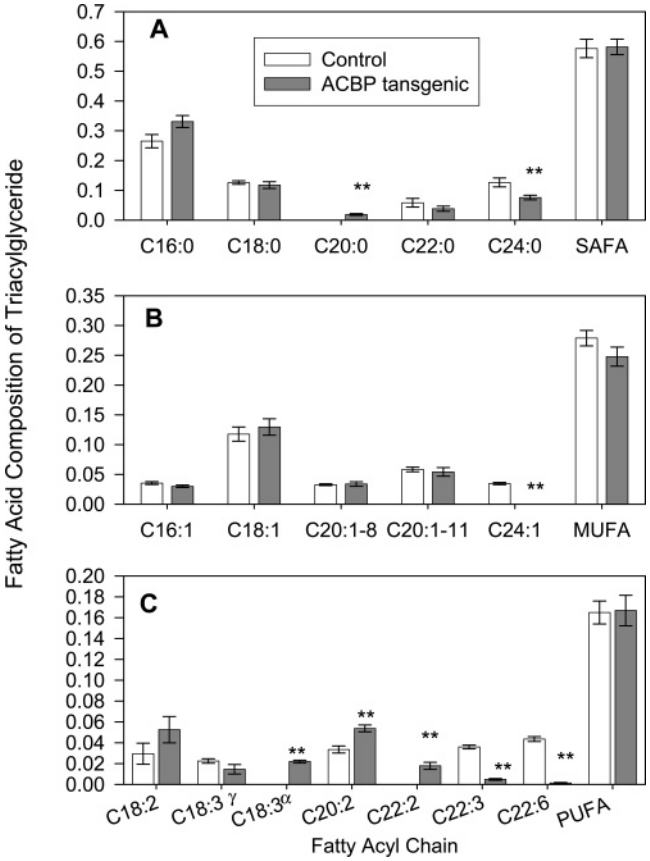

FIGURE 8: Fatty acid composition of triacylglycerides from livers of ACBP transgenic and control mice. Liver lipids were extracted and resolved by TLC. Triacylglyceride spots were hydrolyzed and converted to FAMEs and analyzed by gas chromatography as described in Materials and Methods. The results (mean ± SE; $n = 4-8$) are presented as fatty acid fractions. Panels: A, saturated fatty acids (SAFA); B, monounsaturated fatty acids (MUFA); C, polyunsaturated fatty acids (PUFA). *, **: significantly different from controls (*, $p < 0.05$; **, $p < 0.01$).

mice contain more C20:4 and C22:6 acyl chains, the data presented herein with older mice were consistent with the low amounts of these acyl chains in the liver LCFA-CoA pools of such mice (Figure 5). Taken together, these data suggest that ACBP transgenic mice in general exhibited decreased percent composition of most types of very long chain LCFAs (C24:0, C24:1, C22:3, C22:6) esterified to triacylglycerides.

Activity of Glycerol-3-phosphate Acyltransferase (GPAT), the Key Rate-Limiting Enzyme in Glycerolipid Synthesis, in ACBP Transgenic Mice. Addition of exogenous ACBP is known to enhance the transacylation of LCFA-CoAs into phosphatidic acid in vitro (*39*, *44*, *60*). To test if livers of ACBP transgenic mice also exhibited enhanced LCFA-CoA transacylation, [1-^{14}C]oleoyl-CoA and glycerol 3-phosphate were incubated with cell homogenates of ACBP transgenic and control livers, and the formation of phosphatidic acid was monitored as described in Materials and Methods. In ACBP transgenic mouse liver homogenates, the formation of the radioactive phosphatidic acid was 26.7 ± 2.0 pmol min^{-1} (mg of protein)$^{-1}$, increased >4-fold as compared to that of control livers [6.2 ± 0.5 pmol min^{-1} (mg of protein)$^{-1}$] (Figure 9). Therefore, livers of ACBP transgenic mice had enhanced GPAT activity, consistent with the 2-fold increase in liver phospholipid and triacylglyceride mass in livers of ACBP transgenic mice (Figure 6).

Expression of GPAT, LAT, and ACAT-2 Proteins in Livers of ACBP Transgenic Mice. In the experiments discussed above, it is shown that livers of ACBP transgenic mice had increased GPAT enzymatic activity and an increased amount of liver phosphatidic acid derived glycerides, especially phospholipids and less so triacylglycerides. This effect was specific since the amount of cholesterol ester was unaltered. To differentiate whether the increase in phosphatidic acid derived glycerides was due to the presence of increased amount of ACBP or to increased protein levels of GPAT (rate-limiting enzyme of phosphatidic acid synthesis) or LAT (catalyzes the second, non-rate-limiting step of phosphatidic acid synthesis), Western blotting was used to determine the relative levels of the respective proteins in liver homogenates from ACBP transgenic and control mice. Western blots of liver homogenates from ACBP transgenic mice had no significant alterations in levels of GPAT or LAT proteins (Figure 9). Likewise, Western blots of liver homogenates of ACBP transgenic mice also did not reveal any significant changes in ACAT-2 protein level (Figure 9). These data were

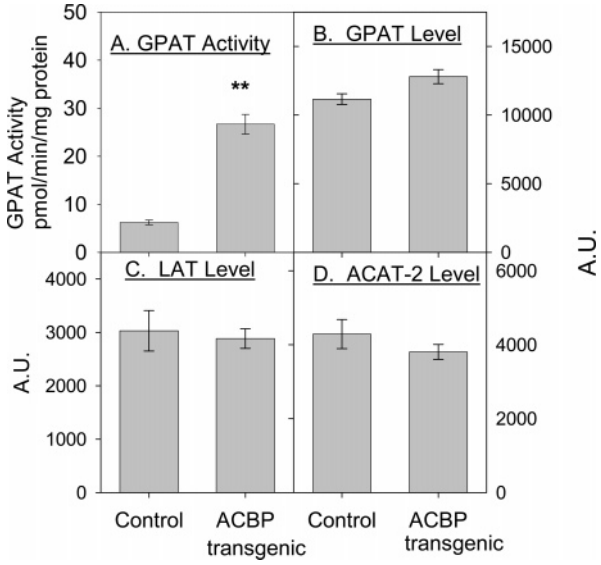

FIGURE 9: Effect of ACBP transgene on liver transacylase enzyme activities and protein levels. Glycerol-3-phosphate acyltransferase, i.e., GPAT (panel A), activity was determined by incubating [1-^{14}C]-oleoyl-CoA, glycerol 3-phosphate, and the liver homogenate of ACBP transgenic or control mice for 15 min, extracting the lipids, separating the lipids on TLC, and counting the radioactivity of the phosphatidic acid spots as described in Materials and Methods. Western blotting and densitometric analysis were used to determine relative protein levels of GPAT (panel B), lysophosphatidic acid acyltransferase (LAT, panel C), and acyl-CoA cholesterol acyltransferase (ACAT-2, panel D) as described in Materials and Methods. Liver homogenates from ACBP transgenic and control mice were run on the same gel. All results are presented as mean ± SE ($n = 3-8$). *, **: significantly different from controls (*, $p < 0.05$; **, $p < 0.01$).

consistent with the elevated mass of glycerolipids (phospholipids, triacylglycerides) and GPAT activity of livers from ACBP transgenic mice being due to the increased level of ACBP, rather than increased level of GPAT or LAT enzyme protein. Likewise, the unaltered levels of cholesteryl esters in the livers of ACBP transgenic mice were not due to the decreased level of ACAT-2 enzyme protein.

DISCUSSION

Although ACBP exhibits high affinity for long-chain fatty acyl-CoAs (LCFA-CoAs), the physiological function of ACBP in mammalian tissues is not yet resolved (reviewed in refs *1*−*5*). ACBP is unique among the various intracellular LCFA-CoA binding proteins in that it exclusively binds only LCFA-CoAs with high affinity (reviewed in refs *1*, *2*, and *30*). By selective interaction with LCFA-CoAs in the cell, ACBP may influence diverse cellular processes in which these ligands are involved. For example, LCFA-CoAs not only serve as metabolic intermediates but are required for glucose uptake (*6*−*12*), vesicular trafficking (*13*−*18*), and signaling (*2*, *19*). Not only are LCFA-CoAs also important for regulation of DNA transcription (*20*−*24*), but nuclear transcription factors involved in fatty acid and glucose metabolism, e.g., HNF4α (*21*) and PPARα (*61*), exhibit a distinct preference for LCFA-CoAs with select chain lengths and degrees of unsaturation (*22*, *29*). Despite the importance of LCFA-CoAs and the high affinity (≤0.5 nM K_d) of ACBP for LCFA-CoA, however, almost nothing is known about whether ACBP affects LCFA-CoA pool size, LCFA-CoA acyl chain composition, LCFA-CoA distribution, glyceride lipid mass, and glyceride lipid acyl chain composition in mammalian tissues. The data presented herein utilized ACBP transgenic mice to begin to address these issues.

First, the increased ACBP expression in ACBP transgenic mice was not due to inappropriate random insertion of the construct. Western blotting of liver homogenates from eight different transgenic lines revealed that all lines had elevated liver ACBP protein with the mean being 1.33-fold increase in liver ACBP protein. Thus, the increased ACBP expression was not due to inappropriate targeting of the ACBP cDNA during the random insertion involved in creating the transgenic mice.

Second, the increased level of ACBP protein in ACBP transgenic mice was in the physiological range. The 33% increased ACBP expression in livers of ACBP transgenic mice was similar to that observed under normal physiological challenges. For example, fasting for 24−48 h decreases liver ACBP levels by 41% while feeding a high fat diet for 48 h increases liver ACBP expression near 50% (*56*). In addition, this increased ACBP level was in the same range as that observed in rodents in response to dietary peroxisome proliferator agents (*57*, *58*) or genetic obesity (*62*). Highly elevated, nonphysiological overexpression of ACBP was avoided because excessive levels of ACBP are associated with (i) malignancy (reviewed in refs *1* and *63*)), (ii) chronic hepatic encephalopathy (reviewed in ref *1*), (iii) behavioral changes (reviewed in ref *1*), and (iv) inhibition, rather than stimulation, of transacylation enzymes in the liver. The latter is evidenced by in vitro studies showing that at low ACBP/LCFA-CoA molar ratios ACBP enhances LCFA-CoA transacylation via GPAT to form phosphatidic acid (*39*) and via ACAT-2 to form cholesterol ester (*5*). In contrast, at high ACBP/LCFA-CoA molar ratios these activities are inhibited (*5*, *39*). Therefore, ACBP transgenic mice were created to increase ACBP expression only to the extent normally observed in response to diet or other normal physiological challenges rather than to excessively high levels in the nonphysiological response range.

Third, livers of ACBP transgenic mice exhibited increased liver LCFA-CoA pool size. The data showed for the first time that increased expression of ACBP in a mammalian system elicited increased LCFA-CoA pool size. As compared to control mice, livers of ACBP transgenic mice contained 69% more LCFA-CoA. This level of increase was in the physiological range in mammals in response to dietary or other interventions (reviewed in refs *1*, *2*, and *19*)). The finding of increased liver LCFA-CoA pool size in ACBP transgenic mice was supported by studies with a single-celled eukaryote, yeast, wherein ACBP overexpression similarly increased LCFA-CoA pool size (*64*). Studies performed in vitro provide a mechanistic basis for these observations: (i) ACBP stimulates LCFA-CoA synthesis (*37*), (ii) ACBP protects LCFA-CoA against hydrolysis by acyl-CoA hydrolases (*1*, *2*, *19*, *37*), and (iii) ACBP removes inhibition of the long-chain acyl-CoA synthetase (lc-ACS) by LCFA-CoA end product. The lc-ACS synthesizes LCFA-CoA from LCFA, CoA, and ATP substrates. However, the end product LCFA-CoA inhibits the enzyme (*65*). By binding LCFA-CoA with high affinity, ACBP is thought to enhance desorption of LCFA-CoA from lc-ACS to significantly stimulate lc-ACS activity (more than doubled the initial rate) by relieving the product inhibition (*37*). Finally, it should

be noted that the increased level of LCFA-CoA (69%) was qualitatively, but not directly, proportional to the increased level of ACBP (33%) in livers of transgenic mice. The basis for the lack of direct quantitative proportionality is not completely clear, but a similar lack of direct quantitative proportionality was noted in a previous study with muscles from genetically obese Zucker rats as compared to control rats (*62*). In the obese Zucker rat, LCFA-CoA is increased 90% while ACBP increases only 30% (*62*). Taken together, the present study is unique in that it showed for the first time that ACBP expression increased LCFA-CoA pool size under physiological conditions in a mammal.

Fourth, livers of ACBP transgenic mice exhibited altered acyl chain composition of LCFA-CoAs. The data showed for the first time that ACBP selectively altered the acyl chain composition of LCFA-CoAs in a physiological context, i.e., liver of ACBP transgenic mice. Increased expression of ACBP significantly increased the liver mass (pmol/mg of protein) of saturated and polyunsaturated LCFA-CoAs, the mass of monounsaturated LCFA-CoAs remained unaltered. The increase in saturated LCFA-CoA mass was consistent with (i) ACBP's higher affinity for saturated LCFA-CoA (especially C14−C20) than monounsaturated LCFA-CoA as shown herein by the *cis*-parinaroyl-CoA displacement assay and by others' use of a covalently modified ACBP (*31*) [while mono- and polyunsaturated LCFA-CoAs were not examined, several early studies also showed that ACBP exhibits high affinity for saturated LCFA-CoAs with C14−C20 acyl chains (*66*, *67*)], (ii) tighter binding resulting in better protection of ACBP-bound saturated LCFA-CoAs from being hydrolyzed by intracellular hydrolases (*39*), and (iii) ACBP overexpression in yeast resulting in a significantly increased level of some saturated LCFA-CoAs (e.g., C16:0-CoA), while the monounsaturated LCFA-CoAs (e.g., C18:1-CoA) were unaltered (*64*).

Interestingly, despite ACBP's lower affinity for polyunsaturated LCFA-CoAs, ACBP expression increased the liver mass of polyunsaturated LCFA-CoAs. Similarly, it was reported that ACBP overexpression in yeast also results in a significantly increased level of polyunsaturated LCFA-CoAs (e.g., C18:2-CoA), while that of the monounsaturated LCFA-CoAs (e.g., C18:1-CoA) remained essentially the same (*64*). While the exact mechanism(s) accounting for these observations remain(s) to be resolved, at least two possibilities may account for the increased level of polyunsaturated LCFA-CoAs in livers of ACBP transgenic mice: (i) ACBP may facilitate LCFA-CoA desaturation. (ii) ACBP is known to directly interact with membranes to donate bound LCFA-CoAs and facilitate their utilization by microsomal lipid synthetic enzymes (*4*, *5*). ACBP may function as a transfer protein that donates the more tightly bound LCFA-CoA substrates (i.e., saturated and monounsaturated LCFA-CoAs) to the active membrane-bound desaturase enzymes. ACBP less efficiently directs the utilization of polyunsaturated LCFA-CoAs by microsomal acyltransferases, thereby resulting in greater accumulation of polyunsaturated LCFA-CoAs in the liver LCFA-CoA pool. Indeed, ACBP most efficiently binds LCFA-CoAs and enhances their utilization by microsomal acyltransferases in the order saturated LCFA-CoAs > monounsaturated LCFA-CoAs > polyunsaturated LCFA-CoAs (*38*, *39*). Further, ACBP enhances the utilization of saturated LCFA-CoAs, the preferred substrate of CPT1 which is the key enzyme for converting LCFA-CoA to LCFA-carnitine for mitochondrial oxidation (*68*, *69*). In summary, ACBP transgenic mice exhibited significantly increased liver mass of LCFA-CoAs containing saturated and, even more so, polyunsaturated acyl chains. These data showed for the first time that not only did increased ACBP expression increase the total mass of liver LCFA-CoAs but this increase was selective for specific types of LCFA-CoAs. The overall effect of increased ACBP selectively increasing the liver polyunsaturated LCFA-CoA mass was evident even when the LCFA-CoA composition was expressed on a percent rather than mass basis.

Fifth, ACBP transgenic mice exhibited increased distribution of LCFA-CoAs to the liver membrane/organelle fraction, especially microsomes, while decreasing its distribution in the liver soluble/cytosolic fraction. Based on in vitro studies alone is difficult a priori to determine whether ACBP would extract LCFA-CoAs from membranes or donate/enhance LCFA-CoA distribution to membranes. In favor of the former possibility, in vitro studies show that ACBP can extract LCFA-CoAs from membranes (*4*, *36*). In contrast, other in vitro data show that ACBP transports bound LCFA-CoA to membranes to donate bound LCFA-CoAs to microsomal lipid synthetic enzymes (*4*, *5*) and organelles wherein LCFA-CoAs are oxidized (*36*). Thus, the in vitro studies suggested that ACBP is able to directly interact with specific membranes, extract membrane-embedded LCFA-CoA, and transfer/donate bound LCFA-CoA to acceptor membranes or organelles with the net effect in a physiological context unknown. The data presented herein showed for the first time that increased ACBP expression increased the distribution of LCFA-CoA to the membrane/organelle fraction, especially microsomes but not mitochondria, while concomitantly reducing that in the soluble/cytosolic fraction of mouse liver. This finding suggests that, although LCFA-CoA levels are generally high in both microsomes and mitochondria (reviewed in ref *1*), increased ACBP expression in the ACBP transgenic mice selectively increased the LCFA-CoA pool size in microsomes but not mitochondria. Taken together, these results suggested that in mouse liver (i) ACBP more efficiently transferred, rather than extracted, bound LCFA-CoAs to liver membranes/organelles and (ii) ACBP delivers bound LCFA-CoA to efficient LCFA-CoA transport systems present in membrane/organelles (e.g., microsomes) to enhance LCFA-CoA accumulation and glyceride (e.g., phosphatidic acid, triacylglycerol) synthesis therein (*70*). The ACBP/LCFA-CoA complex, rather than LCFA-CoA, preferentially donates LCFA-CoA to membranes in in vitro (*4*) transacylase enzymes (*70*) and LCFA-CoA sensitive ion channels (*71*). (iii) ACBP-facilitated transport of LCFA-CoAs to membranes/organelles may result in sufficiently high LCFA-CoA levels to inhibit LCFA-CoA utilizing enzymes therein. However, ACBP inhibits LCFA-CoA utilizing enzymes in vitro only when the soluble/cytosol molar ratio of LCFA-CoA/ACBP ratio is <0.8 (*4*, *5*, *38*, *44*, *45*, *60*, *72*, *73*).

It should be noted that the effect of increased expression of ACBP in ACBP transgenic mice on redistributing liver LCFA-CoAs preferentially to membrane/organelle fraction was consistent with the LCFA-CoA acyl chain specificity of ACBP. The results showed that, in livers of ACBP transgenic mice, the increase in LCFA-CoA level in the

membrane/organelle fraction was in the order saturated > monounsaturated > polyunsaturated LCFA-CoA, which correlated with ACBP's binding affinity. However, this does not exclude the contribution of CPT I and CAT I substrate selectivity on the amount of each type of LCFA-CoA translocated into the mitochondria and microsome interiors.

Sixth, while increased ACBP expression in ACBP transgenic mice had no effects on protein levels of key liver transacylase enzymes (i.e., GPAT, LAT, ACAT-2), increased ACBP expression stimulated liver GPAT activity (i.e., increased the rate of phosphatidic acid synthesis). Since phosphatidic acid is the precursor of de novo synthesis of phospholipids and triacylglycerides, as expected the mass of these glycerides was significantly increased in livers from ACBP transgenic mice. While ACBP transgenic mice clearly also exhibited altered acyl chain composition of the liver phospholipids and triacylglycerides, which together account for the majority of esterified lipid, a universal pattern of select acyl changes was not observed. For example, the fact that the monounsaturated C18:1 fatty acid content was increased in the liver phospholipid fraction of ACBP transgenic mice appeared consistent with several factors: (i) ACBP's higher affinity for saturated LCFA-CoAs as shown herein and earlier (*30*), (ii) ACBP's inhibition of saturated LCFA-CoA transacylation to form phosphatidic acid (*39*) [ACBP stimulated GPAT activity and altered the fatty acyl-CoA selectivity of microsomal phosphatidic acid synthesis in the following order: oleoyl-CoA (a monounsaturated acyl-CoA) > arachidonoyl-CoA (a polyunsaturated acyl-Coa) ≫ palmitoyl-CoA (a saturated fatty acyl-CoA whose transacylation was actually inhibited by ACBP), and ACBP only weakly (10%) stimulated microsomal LAT if at all (*39*)], and (iii) ACBP's preferential targeting of saturated LCFAs to mitochondria for oxidation (*69*). On the other hand, regardless of the degree of unsaturation, the content of some of the very long chain LCFAs was preferentially decreased in the liver phospholipids and even more so in triacylglycerides of ACBP transgenic mice. This pattern may be explained in part by ACBP's relatively weaker binding affinity for LCFA-CoAs with chain lengths >C20 (*31*) or, alternately, other unknown factors not related to ACBP affinity for specific LCFA-CoA species.

In summary, the data presented herein with ACBP transgenic mice established for the first time in a mammalian system and more physiological context that increased ACBP expression increased the liver LCFA-CoA pool size, elicited preferential accumulation of polyunsaturated LCFA-CoAs, and preferentially distributed LCFA-CoAs to the membrane/organelle fraction (especially microsomes) in accordance with ACBP's specificity for select LCFA-CoAs. While livers of ACBP transgenic mice exhibited unaltered protein levels of GPAT, LAT, and ACAT-2, nevertheless liver GPAT activity was stimulated, phospholipid and triglyceride masses were increased, and the acyl chain compositions of both phospholipids (increased the monounsaturated C18:1) and triacylglycerides were altered. Thus, the data presented herein for the first time demonstrate the physiological relevance of ACBP in determining LCFA-CoA parameters and acylation to glycerides in a mammalian system.

REFERENCES

1. Gossett, R. E., Frolov, A. A., Roths, J. B., Behnke, W. D., Kier, A. B., and Schroeder, F. (1996) Acyl Co A binding proteins: multiplicity and function, *Lipids 31*, 895−918.
2. Faergeman, N. J., and Knudsen, J. (1997) Role of long-chain fatty acyl-CoA esters in the regulation of metabolism and in cell signalling, *Biochem. J. 323*, 1−12.
3. Chao, H., Billheimer, J. T., Kier, A. B., and Schroeder, F. (1999) Microsomal long chain fatty acyl CoA transacylation: differential effect of SCP-2, *Biochim. Biophys. Acta 1439*, 371−383.
4. Chao, H., Martin, G., Russell, W. K., Waghela, S. D., Russell, D. H., Schroeder, F., and Kier, A. B. (2002) Membrane charge and curvature determine interaction with acyl CoA binding protein (ACBP) and fatty acyl CoA targeting, *Biochemistry 41*, 10540−10553.
5. Chao, H., Zhou, M., McIntosh, A., Schroeder, F., and Kier, A. B. (2002) Acyl CoA binding protein and cholesterol differentially alter fatty acyl CoA utilization by microsomal acyl CoA: cholesterol transferase, *J. Lipid Res. 44*, 72−83.
6. McGarry, J. D., and Dobbins, R. L. (1999) Fatty acids, lipotoxicity, and insulin secretion, *Diabetologia 42*, 128−138.
7. Antinozzi, P. A., Segall, L., Prentki, M., McGarry, J. D., and Newgard, C. B. (1998) Molecular or pharmacologic perturbation of the link between glucose and lipid metabolism is without effect on glucose-stimulated insulin secretion, *J. Biol. Chem. 273*, 16146−16154.
8. Prentki, M., Vischer, S., Glennon, M. C., Regazzi, R., Deeney, J. T., and Corkey, B. E. (1992) Malonyl-CoA and long chain acyl-CoA esters as metabolic coupling factors in nutrient-induced insulin secretion, *J. Biol. Chem. 267*, 5802−5810.
9. Larsson, O., Deeney, J. T., Branstrom, R., Berggren, P. O., and Corkey, B. E. (1996) *J. Biol. Chem. 271*, 10623−10626.
10. Shimabukuro, M., Levi, M., and Unger, R. H. (1998) Fatty acid-induced beta cell apoptosis: a link between obesity and diabetes, *Proc. Natl. Acad. Sci. U.S.A. 95*, 2498−2502.
11. Chen, Z.-W., Agerberth, B., Gell, K., Andersson, M., Mutt, V., Ostenson, C.-G., Efendic, S., Barros-Soderling, J., Persson, B., and Jörnvall, H. (1988) Isolation and characterization of porcine diazepam-binding inhibitor, a polypeptide not only of cerebral occurrence but also common in intestinal tissues and with effects on regulation of insulin release, *Eur. J. Biochem. 174*, 239−245.
12. Ostenson, C.-G., Ahren, B., Karlsson, S., Knudsen, J., and Efendic, S. (1994) Inhibition by rat diazepam-binding inhibitor/acyl-CoA-binding protein of glucose-induced insulin secretion in the rat, *Eur. J. Endocrinol. 131*, 201−204.
13. Glick, B. S., and Rothman, J. E. (1987) Possible role for fatty acyl-coenzyme A in intracellular protein transport, *Nature 326*, 309−312.
14. Pfanner, N., Orci, L., Glick, B. S., Amherdt, M., Arden, S. R., Malhotra, V., and Rothman, J. E. (1989) Fatty acyl CoA is required for budding of transport vesicles from Golgi cisternae, *Cell 59*, 95−102.
15. Pfanner, N., Glick, B. S., Arden, S. R., and Rothman, J. E. (1990) Fatty acylation promotes fusion of transport vesicles with Golgi cisternae, *J. Cell Biol. 110*, 955−961.
16. Weigert, R., Silletta, M. G., Spano, S., Turacchio, G., Cericola, C., Colanzi, A., Senatore, S., Mancini, R., Polishchuk, E. V., Salmona, M., Facchiano, F., Burger, K. N. J., Mironov, A., Luini, A., and Corda, D. (1999) CtBP/BARS induces fission of Golgi membranes by acylating lysophosphatidic acid, *Nature 402*, 429−433.
17. Schmidt, A., Wolde, M., Thiele, C., Fest, W., Kratzin, H., Podtelejnikov, A. V., Witke, W., Huttner, W. B., and Soling, H.-D. (1999) Endophilin mediates vesicle formation by transfer of arachidonate to lysophosphatidic acid, *Nature 401*, 133−141.
18. Gaigg, B., Neergard, T. B., Schneiter, R., Hansen, J. K., Faergeman, N. J., Jensen, N. A., Andersen, J. R., Friis, J., Sandhoff, K., and Knudsen, J. (2001) Depletion of acyl CoA binding protein affects sphingolipid synthesis and causes vesicle accumulation and membrane defects in *S. cerevisiae*, *Mol. Biol. Cell 12*, 1147−1160.
19. Knudsen, J., Jensen, M. V., Hansen, J. K., Faergeman, N. J., Neergard, T., and Gaigg, B. (1999) Role of acyl CoA binding protein in acyl CoA transport, metabolism, and cell signaling, *Mol. Cell. Biochem. 192*, 95−103.
20. Raman, N., Black, P. N., and DiRusso, C. C. (1997) Characterization of the fatty acid responsive transcription factor FadR

biochemical and genetic analyses of native conformation and functional domains, *J. Biol. Chem. 272*, 30645−30646.
21. Hertz, R., Magenheim, J., Berman, I., and Bar-Tana, J. (1998) Fatty acyl-CoA thioesters are ligands of hepatic nuclear factor-4a, *Nature 392*, 512−516.
22. Hertz, R., Sheena, V., Kalderon, B., Berman, I., and Bar-Tana, J. (2001) Suppression of hepatocyte nuclear factor 4alpha by acyl-CoA thioesters of hypolipidemic peroxisome proliferators, *Biochem. Pharmacol. 61*, 1057−1062.
23. Petrescu, A. D., Hertz, R., Bar-Tana, J., Schroeder, F., and Kier, A. B. (2002) Ligand specificity and conformational dependence of the hepatic nuclear factor-4alpha (HNF-4a), *J. Biol. Chem. 277*, 23988−23999.
24. Hertz, R., Ben-Haim, M., Petrescu, A., Kalderon, B., Berman, I., Eldad, N., Schroeder, F., and Bar-Tana, J. (2003) Rescue of MODY-1 by agonist ligands of HNF4alpha, *J. Biol. Chem. 278*, 22578−22585.
25. McArthur, M. J., Atshaves, B. P., Frolov, A., Foxworth, W. D., Kier, A. B., and Schroeder, F. (1999) Cellular uptake and intracellular trafficking of long chain fatty acids, *J. Lipid Res. 40*, 1371−1383.
26. Wolfrum, C., Borrmann, C. M., Borchers, T., and Spener, F. (2001) Fatty acids and hypolipidemic drugs regulate PPARalpha and PPARgamma gene expresion via L-FABP: a signaling path to the nucleus, *Proc. Natl. Acad. Sci. U.S.A. 98*, 2323−2328.
27. Schroeder, F., Atshaves, B. P., Starodub, O., Boedeker, A. L., Smith, R., Roths, J. B., Foxworth, W. B., and Kier, A. B. (2001) Expression of liver fatty acid binding protein alters growth and differentiation of embryonic stem cells, *Mol. Cell. Biochem. 219*, 127−138.
28. Huang, H., Starodub, O., McIntosh, A., Atshaves, B. P., Woldegiorgis, G., Kier, A. B., and Schroeder, F. (2004) Liver fatty acid binding protein colocalizes with peroxisome proliferator receptor alpha and enhances ligand distribution to nuclei of living cells, *Biochemistry 43*, 2484−2500.
29. Petrescu, A. D., Payne, H. R., Boedeker, A. L., Chao, H., Hertz, R., Bar-Tana, J., Schroeder, F., and Kier, A. B. (2003) Physical and functional interaction of acyl CoA binding protein (ACBP) with hepatocyte nuclear factor-4alpha (HNF4alpha), *J. Biol. Chem. 278*, 51813−51824.
30. Frolov, A. A., and Schroeder, F. (1998) Acyl coenzyme A binding protein: conformational sensitivity to long chain fatty acyl-CoA, *J. Biol. Chem. 273*, 11049−11055.
31. Wadum, M. C. T., Villadsen, J. K., Feddersen, S., Moller, R. S., Neergaard, T. B. F., Kragelund, B. B., Hojrup, P., Faergeman, N. J., and Knudsen, J. (2002) Fluorescently labelled bovine acyl CoA binding protein acting as an acyl CoA sensor: interaction with CoA and acyl CoA esters and its use in measuring free acyl CoA esters and non-esterified fatty acids, *Biochem. J. 365*, 165−172.
32. Jorgensen, C., Krogsdam, A.-M., Kratchamarova, I., Willson, T. M., Knudsen, J., Mandrup, S., and Kristiansen, K. (2002) Opposing effects of fatty acids and acyl-CoA esters on conformation and cofactor recruitment of peroxisome proliferator activated receptors, *Ann. N.Y. Acad. Sci. 967*, 431−439.
33. Frolov, A., Cho, T. H., Murphy, E. J., and Schroeder, F. (1997) Isoforms of rat liver fatty acid binding protein differ in structure and affinity for fatty acids and fatty acyl CoAs, *Biochemistry 36*, 6545−6555.
34. Frolov, A., Cho, T. H., Billheimer, J. T., and Schroeder, F. (1996) Sterol carrier protein-2, a new fatty acyl coenzyme A-binding protein, *J. Biol. Chem. 271*, 31878−31884.
35. Schjerling, C. K., Hummel, R., Hansen, J. K., Borsting, C., Mikkelsen, J., Kristiansen, K., and Knudsen, J. (1996) Disruption of the gene encoding the acyl-CoA-binding protein (ACB1) perturbs acyl-CoA metabolism in *Saccharomyces cerevisiae*, *J. Biol. Chem. 271*, 22514−22521.
36. Rasmussen, J. T., Faergeman, N. J., Kristiansen, K., and Knudsen, J. (1994) Acyl-CoA-binding protein (ACBP) can mediate intermembrane acyl-CoA transport and donate acyl-CoA for beta-oxidation and glycerolipid synthesis, *Biochem. J. 299*, 165−170.
37. Rasmussen, J. T., Rosendal, J., and Knudsen, J. (1993) Interaction of acyl-CoA binding protein (ACBP) on processes for which acyl-CoA is a substrate, product or inhibitor, *Biochem. J. 292*, 907−913.
38. Gossett, R. E., Edmondson, R. D., Jolly, C. A., Cho, T. H., Russell, D. H., Knudsen, J., Kier, A. B., and Schroeder, F. (1998) Structure and function of normal and transformed murine acyl CoA binding proteins, *Arch. Biochem. Biophys. 350*, 201−213.
39. Jolly, C. A., Wilton, D. A., and Schroeder, F. (2000) Microsomal fatty acyl CoA transacylation and hydrolysis: fatty acyl CoA species dependent modulation by liver fatty acyl CoA binding proteins, *Biochim. Biophys. Acta 1483*, 185−197.
40. Knudsen, J., Faergeman, N. J., Skott, H., Hummel, R., Borsting, C., Rose, T. M., Andersen, J. S., Hojrup, P., Roepstorff, P., and Kristiansen, K. (1994) Yeast acyl-CoA-binding protein: acyl-CoA-binding affinity and effect on intracellular acyl-CoA pool size, *Biochem. J. 302*, 479−485.
41. (1994) Production of transgenic mice, in *Manipulating the mouse embryo, a laboratory manual* (Hogan, B., Beddington, R., Costantini, F., and Lacy, E., Eds.) pp 217−252, Cold Spring Harbor Laboratory Press, Plainview, NY.
42. Woldegiorgis, G., Spennetta, T., Corkey, B. E., Williamson, J. R., and Shrago, E. (1985) Extraction of tissue long-chain acyl-CoA esters and measurement by reverse-phase high-performance liquid chromatography, *Anal. Biochem. 150*, 8−12.
43. Olbrich, A., Dietl, B., and Lynen, F. (1981) Determination and characterization of long-chain fatty acyl-CoA thioesters from yeast and mammalian liver, *Anal. Biochem. 113*, 386−397.
44. Jolly, C. A., Hubbell, T., Behnke, W. D., and Schroeder, F. (1997) Fatty acid binding protein: Stimulation of microsomal phosphatidic acid formation, *Arch. Biochem. Biophys. 341*, 112−121.
45. Jolly, C. A., Murphy, E. J., and Schroeder, F. (1998) Differential influence of rat liver fatty acid binding protein isoforms on phospholipid fatty acid composition: phosphatidic acid biosynthesis and phospholipid fatty acid remodeling, *Biochim. Biophys. Acta 1390*, 258−268.
46. Gallegos, A. M., Atshaves, B. P., Storey, S., McIntosh, A., Petrescu, A. D., and Schroeder, F. (2001) Sterol carrier protein-2 expression alters plasma membrane lipid distribution and cholesterol dynamics, *Biochemistry 40*, 6493−6506.
47. Bradford, M. (1976) A rapid and sensitive method for the quantitation of microgram quantities of protein utilizing the principle of protein dye binding, *Anal. Biochem. 72*, 248−254.
48. Schägger, H., and Von Jagow, G. (1987) Tricine-sodium dodecyl sulfate-polyacrylamide gel electrophoresis for the separation of proteins in the range from 1 to 100 kDa, *Anal. Biochem. 166*, 368−379.
49. Atshaves, B. P., Storey, S., McIntosh, A. L., Petrescu, A. D., Lyuksyutova, O. I., Greenberg, A. S., and Schroeder, F. (2001) Sterol carrier protein-2 expression modulates protein and lipid composition of lipid droplets, *J. Biol. Chem. 276*, 25324−25335.
50. Powell, G. L., Tippett, P. S., Kiorpes, T. C., McMillin-Wood, J., Coll, K. E., Schultz, H., Tanaka, K., Kang, E. S., and Shrago, E. (1985) Fatty acyl CoA as an effector molecule in metabolism, *Fed. Proc. 44*, 81−84.
51. Larson, T. R., and Graham, I. A. (2001) A novel technique for the sensitive quantification of fatty acyl CoA esters from plant tissues, *Plant J. 25*, 115−125.
52. Golovko, M. Y., and Murhpy, E. J. (2004) An improved method for tissue long chain acyl CoA extraction and analysis, *J. Lipid Res. 45*, 1777−1782.
53. Atshaves, B. P., Payne, H. R., McIntosh, A. L., Tichy, S. E., Russell, D., Kier, A. B., and Schroeder, F. (2004) Sexually dimorphic metabolism of branched chain lipids in C57BL/6J mice, *J. Lipid Res. 45*, 812−830.
54. Martin, G. G., Huang, H., Atshaves, B. P., Binas, B., and Schroeder, F. (2003) Ablation of the liver fatty acid binding protein gene decreases fatty acyl CoA binding capacity and alters fatty acyl CoA pool distribution in mouse liver, *Biochemistry 42*, 11520−11532.
55. Marzo, A., Ghirardi, P., Sardini, D., and Meroni, G. (1971) Simplified measurement of monoglycerides, diglycerides, triglycerides, and free fatty acids in biological samples, *Clin. Chem. 17*, 145−147.
56. Bhuiyan, J., Pritchard, P. H., Pande, S. V., and Seccombe, D. W. (1995) Effects of high-fat diet and fasting on levels of acyl-coenzyme A binding protein in liver, kidney, and heart of rat, *Metabolism 44*, 1185−1189.
57. Sterchele, P. F., Vanden Heuvel, J. P., Davis, J. W., Shrago, E., Knudsen, J., and Peterson, R. E. (1994) Induction of hepatic acyl-CoA-binding protein and liver fatty acid-binding protein by perfluorodecanoic acid in rats. Lack of correlation with hepatic long-chain acyl-CoA levels, *Biochem. Pharmacol. 48*, 955−966.
58. Vanden Heuvel, J. P., Sterchele, P. F., Nesbit, D. J., and Peterson, R. E. (1993) Coordinate induction of acyl-CoA binding protein, fatty acid binding protein and peroxisomal b-oxidation by peroxisome proliferators, *Biochim. Biophys. Acta 1177*, 183−190.

59. Atshaves, B. P., McIntosh, A. L., Payne, H. R., Mackie, J., Kier, A. B., and Schroeder, F. (2005) Effect of branched-chain fatty acid on lipid dynamics in mice lacking liver fatty acid binding protein gene, *Am. J. Physiol. 288*, C543−C558.
60. Schroeder, F., Jolly, C. A., Cho, T. H., and Frolov, A. A. (1998) Fatty acid binding protein isoforms: structure and function, *Chem. Phys. Lipids 92*, 1−25.
61. Hostetler, H. A., Petrescu, A. D., Kier, A. B., and Schroeder, F. (2005) Peroxisome proliferator activated receptor alpha (PPA-Ralpha) interacts with high affinity and is conformationally responsive to endogenous ligands, *J. Biol. Chem. 280*, 18667−18682.
62. Franch, J., Knudsen, J., Ellis, B. A., Pedersen, P. K., Cooney, G. J., and Jensen, J. (2002) Acyl CoA binding protein expression is fiber type-specific and elevated in muscles from the obese insulin-resistant Zucker rat, *Diabetes 51*, 449−454.
63. Gossett, R. E., Schroeder, F., Gunn, J. M., and Kier, A. B. (1997) Expression of fatty acyl CoA binding proteins in colon cells: response to butyrate and transformation, *Lipids 32*, 577−585.
64. Mandrup, S., Jepsen, R., Skott, H., Rosendal, J., Hojrup, P., Kristiansen, K., and Knudsen, J. (1993) Effect of heterologous expression of acyl-CoA-binding protein on acyl-CoA level and composition in yeast, *Biochem. J. 290*, 369−374.
65. Pande, S. V. (1973) Reversal by CoA of palmityl-CoA inhibition of long chain acyl-CoA synthetase activity, *Biochim. Biophys. Acta 306*, 15−20.
66. Milne, K. G., and Ferguson, M. A. J. (2000) Cloning, expression, and characterization of the acyl-CoA binding protein in African trypanosomes, *J. Biol. Chem. 275*, 12503−12508.
67. Faergeman, N. J., Sigurskjold, B. W., Kragelund, B. B., Andersen, K. V., and Knudsen, J. (1996) Thermodynamics of ligand binding to acyl-coenzyme A binding protein studied by titration calorimetry, *Biochemistry 35*, 14118−14126.
68. Fraser, F., Corstorphine, C. G., Price, N. T., and Zammit, V. A. (1999) Evidence that carnitine palmitoyltransferase I (CPT I) and microsomal carnitine acyltransferase I (CAT I) regulate the entry of fatty acyl moieties into their respective organelle by catalyzing the conversion of LCFA-CoAs into the corresponding acylcarnitines, *FEBS Lett. 446*, 69−74.
69. Woldegiorgis, G., Bremer, J., and Shrago, E. (1985) Substrate inhibition of carnitine palmitoyltransferase by palmitoyl-CoA and activation by phospholipids and proteins, *Biochim. Biophys. Acta 837*, 135−140.
70. Abo-Hashema, K. A. H., Cake, M. H., and Knudsen, J. (1999) Evaluation of the affinity and turnover number of both hepatic mitochondrial and microsomal carnitine acyltransferases: relevance to intracellular partitioning of acyl-CoAs, *Biochemistry 38*, 15840−15847.
71. Fulceri, R., Knudsen, J., Giunti, R., Volpe, P., Nori, A., and Benedetti, A. (1997) Fatty acyl CoA-acyl CoA binding protein complexes activate the Ca^{++} channel of skeletal muscle sarcoplasmic reticulum, *Biochem. J. 325*, 423−428.
72. Jolly, C. A., Chao, H., Kier, A. B., Billheimer, J. T., and Schroeder, F. (2000) Sterol carrier protein-2 suppresses microsomal acyl CoA hydrolysis, *Mol. Cell. Biochem. 205*, 83−90.
73. Bordewick, U., Heese, M., Borchers, T., Robenek, H., and Spener, F. (1989) Compartmentation of hepatic fatty-acid-binding protein in liver cells and its effect on microsomal phosphatidic acid biosynthesis, *Biol. Chem. Hoppe-Seyler 370*, 229−238.

BI0477891